# TWO THEORETICAL STUDIES INVESTIGATING PREDATOR-PREY INTERACTIONS

A Dissertation

Presented to the Faculty of the Graduate School

of Cornell University

in Partial Fulfillment of the Requirements for the Degree of

Doctor of Philosophy

by

Rebecca Jean Tien

February 2010

TWO THEORETICAL STUDIES INVESTIGATING PREDATOR-PREY INTERACTIONS

Rebecca Jean Tien, Ph.D.

Cornell University 2010

This thesis consists of two projects looking at different aspects of predator-prey relationships. The first project examines this relationship in the context of predator-prey coevolution and assumes that the cost for prey defense is variable. The second project looks at ecosystem shifts in the 1990s in the Gulf of Maine and the relative role of top-down verses bottom-up processes on controlling *Calanus finmarchicus* abundance.

**Predator-Prey Coevolution**

Predation can act as a selective pressure which drives prey to adapt a defensive trait to avoid attack. At the same time, predators can evolve a counter-defense which aids them in continued successful attacks. Allocation towards either trait can be costly, in the form of a decrease in fecundity. There is some evidence to suggest that, for the prey at least, cost can vary depending on the level of intra-specific competition. Here we investigated the effects of variable prey trait cost and genetic variability of the predator and prey, on the stability and dynamics of the system. We compared two models, one which assumed that cost of prey defense is fixed, and one that assumed that cost varies proportional to population density. We found that under most conditions, variable cost of prey defense is more stabilizing to the interaction than fixed cost.

**Gulf of Maine Ecosystem**

In the Gulf of Maine in the 1990s an increase in freshwater was associated

with increased phytoplankton blooms, particularly in autumn. This in turn led to increased abundance in most copepods. *Calanus finmarchicus*, one of the most abundant zooplankton species in the region, demonstrated an increase in abundance in the earlier developmental stages but a paradoxical decrease in abundance of the later copepodid stages. At the same time, adult herring, which preferentially feed on late-stage *C. finmarchicus*, increased in abundance by one order of magnitude. Through ordinary differential equation models, we investigated whether increased presence of herring in the 1990s was large enough to contribute to the decline in late-stage *C. finmarchicus*. Additionally, we incorporated food-dependent growth into the later copepodid classes to investigate the impact of phytoplankton variation on the observed shifts in zooplankton abundance.

## BIOGRAPHICAL SKETCH

Rebecca Tien began her academic career as an undergraduate at the State University of New York at New Paltz where she received a B.A. in Psychology and a minor in mathematics in 1998. After some time off for reflection on her future direction of study, in 2002 she began graduate work in the Applied Math department at the Universtiy of Washington in Seattle. Rebecca finished her M.S. in 2004 and directly began her Ph.D. work in the department of Ecology and Evolutionary Biology at Cornell University in Ithaca, NY. The requirements for completion of her dissertation were finished in the fall of 2009. She is currently at the Mathematical Biosciences Institute at Ohio State University in Columbus where she will remain for a two year, NSF-funded postdoctoral fellowship position.

I would like to dedicate this to my family members for tirelessly supporting me along the way: Joseph Tien, Paula Jacobs, Anna Kelles, Jenny and Matt Miller and Dennis and Darrelle Dore.

## ACKNOWLEDGEMENTS

Thank you to my committee members: Stephen Ellner (advisor), Nelson Hairston (co-advisor), and Andrew Pershing. I would also like to thank my labmates and Lunch Bunch members for the many engaging conversations and moral support, including: Laura Jones, Take Yoshida, Lutz Becks, Joe Simonis, Paul Hurtado, Virginia Passeur, Elise Zipken, Ben Hamilton, Michael Cortez. For training in MATCONT and editing help, I would like to thank Joseph Tien. Funding for this dissertation has come from a Cornell Graduate Fellowship, The Andrew Mellon Foundation, and The James S. McDonnell Foundation. This dissertation could not have been completed without the help of the entire administrative staff in the Department of Ecology and Evolutionary Biology, including: Alberta Jackson, Carol Damm, Delores Albertsman, Patty Jordan, Janine Orr, and Brian Mlodsinski for keeping my various computers running. Thank you!

## TABLE OF CONTENTS

## LIST OF TABLES

## LIST OF FIGURES

CHAPTER 1

# COEVOLUTION AND VARIABLE COST OF PREY DEFENSE IN A PREDATOR-PREY SYSTEM

## 1.1 Abstract

Under certain conditions, predation acts as a selective pressure that drives prey adaptation. In response, the predator can evolve counter-defenses to increase the likelihood of successful attack. Investment in such traits is often costly, so that a trade-off exists between trait investment and competitive ability. There is some evidence that cost, at least for the prey, can vary with changes in the environment such as low resource availability. For our investigation, we assume that competition for resources is most likely to occur at high prey densities. Resource limitation is then synonymous with high prey density in our model although that is not necessarily the case in nature. We investigated the effects of variable prey trait cost and genetic variability of both the predator and prey, on the stability and dynamics of the system. The cost of prey defense is set proportional to prey population density so that, as prey density increases, so does the cost of prey defense. This model is contrasted with the case where prey defense cost is assumed to be density-independent. In both models, the cost for investment in a particular trait is defined as a decrease in fecundity. Quantitative trait models are employed to examine the effect of fixed versus variable cost on both population and trait dynamics. One important assumption of quantitative trait models is the allowance of polymorphisms within the population. This implies that an increase in the amount of total genetic variation in a population will increase the rate at which evolution is occurring. Each model is a system of four differential equations: two

describing predator and prey densities and two which track the mean predator and prey trait values through time. For both models, we assumed that predator counter-defense cost is always fixed. The dynamics of the system were determined through bifurcation analysis and numerical simulation. It was found that under most conditions variable cost of prey defense is more stabilizing than fixed cost. The dynamics of the fixed cost model approach the Rosenzweig-MacArthur model dynamics when genetic variation of both populations is small (i.e. evolution is occurring slowly relative to the ecology), but stability increases with an increase in genetic variation. Stability of the variable cost model is non-monotonic as the amount of genetic variation increases. This system is quite stable at very fast or very slow evolutionary speeds, but less stable at intermediate rates of evolution. It is particularly interesting to note the stabilizing effect of variable prey cost when the amount of genetic variation approaches zero. This suggests that even when evolution is slow, evolution can still have a significant impact on the ecological dynamics of the system.

## 1.2 Introduction

In classic predator-prey models, the coupled population dynamics of the interaction are well understood, but often, the simplifying assumption of homogeneous predator and prey populations is made. In the last few decades ecologists have begun to recognize that genetic variation within prey and predator populations can have a significant impact on population dynamics (1). Predation often acts as a selective pressure, thereby driving prey adaptation. An increase in anti-predator defense capability of the prey may in turn impose a selective pressure on predators to develop a counter-defense, thus leading to a co-evolutionary interaction (4; 19).

One reason for the exclusion of evolution in early predator-prey models was the belief that evolution occurred on a much slower time scale than the ecology and therefore did not impact the ecological dynamics. However, recent experimental evidence suggests that evolution can be quite rapid (28; 5; 40; 27; 16). By this we mean that evolution can happen within a few generations (14). Furthermore, the relative time scale of ecological and evolutionary dynamics can play an important role in determining the stability of the interaction. Yamauchi & Yamamura (2005) for example, found that in a two-prey-one-predator model, increasing additive genetic variance (i.e. increasing the rate of defense evolution) tended to stabilize the interaction (38). In a series of modeling and experimental studies (34; 40; 41; 17) investigated a predator-prey microcosm with rotifers, *Brachionus calyciflorus*, and their algal prey, *Chlorella vulgaris*. It was shown that rapid prey-evolution led to evolutionary (long period, out-of-phase) cycles which did not exist when algae populations were homogeneous and undefended.

Although there is currently little doubt among ecologists that evolution is an important driver of population dynamics, there is some disagreement as to the

mechanism by which evolution occurs. Adaptive Dynamics for example (23; 13; 9) assumes that evolutionary change is a result of the appearance of rare mutations that have an advantage in the ecological setting. A mutation allows the prey to escape from an attack by the predator, who can in turn have a corresponding adaptive mutation that allows for continued attacks. The result is an undending evolutionary arms race. This type of escalatory interaction, in which the predator and prey are essentially "running to stay in the same place", is referred to as Red Queen Dynamics (36; 10).

An underlying assumption of Adaptive Dynamics is that the relevant phenotypic traits are boundless in their evolutionary capability (7; 11). Given that investment in a particular trait can be quite costly, this assumption is perhaps unreasonable. If there were no costs associated with defense for example, we would expect that the trait would sweep to fixation within the population. However, the fact that heritable variation in resistance is often maintained within a population indicates that there is in fact a cost associated with defense (18). According to models which describe coevolution in host-parasitoid interactions (12; 33), whether the system cycles or not depends not only on the ecological advantage of both defense and counter-defense traits, but also on the cost for maintaining each trait. When the cost of resistance against parisitism is high and the cost of parasitoid virulence is low, then one or both populations go extinct. If costs are high for both host and parasitoid, then the host trades off parasitoid resistance in exchange for an increase in fecundity. The parasitoid however continues to invest in search efficiency and stable equilibria are obtained for both traits. If the costs for both traits are intermediate, then simultaneous population and coevolutionary cycles occur.

All organisms experience competing resource demands. An investment in any

particular function inherently implies there are less resources available for allocation to other functions. It is therefore not unreasonable to assume that investment in a defense (or any other trait) might be costly to an organism. However, variations in the environment might impact just how costly a particular trait is. Several studies have found a close link between environmental stress (such as resource limitation) and cost of defense (4). Kraaijeveld and Godfray (1997) investigated a system involving *Drosophila melanogaster* and *Asobara tabida* in which the host, *D. melanogaster*, can evolve resistance from its parasitoid by developing haemocytes which encapsulate the larval *A. tabida* (18). *D. melanogaster* that were able to resist parasitoid attacks showed no difference in growth rate and development time compared to non-resistant types when resources were abundant. As resource limitation increased however, resistant types were out-competed by the non-resistant *D. melanogaster*. This is consistent with the idea that the cost for investment in defense is affected by environmental stress.

As a counter-response to the defense mechanism of *D. melanogaster*, parasitoids can avoid host defenses by hiding their eggs in regions of tissue undetectable by the host haemocytes (18; 19). Again, this counter-defense does not come without a penalty. Embedding the eggs within the tissue wall leads to a delay in egg-hatching. This can prove fatal if the host is attacked by a second species of parasitoid, such as *Leptopilina heterotoma*. If the egg of this competing species hatches first, it will kill *A. tabida* before it has had a chance to emerge.

A recent chemostat experiment by (39), also showed that the cost of prey defense could be variable depending on the amount of available resources. In the absence of their rotifer predator, both defended and undefended algal clones showed little difference in growth rates when resources were abundant. However, when the

amount of resources was limited, the defended clones exhibited a marked decrease in fecundity relative to the undefended clones. In this case, because a trade-off existed between defense and competitive ability, both the prey and the predator densities affected whether it was beneficial to be defended against predation. The result was a direct feedback loop between the evolutionary response of the prey and the densities of both the predator and the prey.

Our research is motivated by experimental evidence that the cost for prey defense is variable, becoming high under stressful conditions, but undetectable when conditions are good. There is evidence that a cost for predator counter-defense can also exist (19). We investigate the dynamics of a coevolutionary system where costs for defense and counter-defense exist, and the cost of prey defense is density-dependent. It is not always the case that variations in density are synonymous with variations in resource limitation. However, we make that simplifying assumption here because we are not explicitly modeling resource availability.

We are interested in the affect of variable cost of prey defense on both the population and trait dynamics of this predator-prey system. We begin by describing two variations of the model, one in which the cost of prey defense is directly proportional to prey density (variable cost model) and one in which the cost is invariant through time (fixed cost model). We assume this linear relationship between prey defense cost and prey density in the variable cost model as a simple starting point although other formulations are possible (e.g. defense cost is a saturating function of prey density). We examine the stability of both models over a wide range of parameter values to determine how the definition of prey defense cost affects the types of dynamics exhibited in each system. We find that under a broad range of parameters the variable cost model is much more stable than the fixed cost model.

## 1.3 Description of the Model

### 1.3.1 Ecological Dynamics

The framework for the current models originates from the basic ecological model developed by (30) in which prey grow logistically (i.e. self-limitation at high densities) and predators have a saturating functional response. The ecological model is modified by adding anti-predator defense in the prey and counter-defense in the predator. These traits are allowed to evolve, so that both the ecological and the evolutionary dynamics change through time. Prey and predator populations experience a cost for investment in defense which is expressed as a decrease in the growth rate of the populations. The only difference between the variable cost and the fixed cost model is how the cost of prey defense is defined.

The resulting models are each a system of four ordinary differential equations, two of which describe the ecological dynamics and two of which track the mean prey and predator trait values. In the following equations, $n$ and a $p$ represent the prey and predator populations, $x$ and $y$ represent the prey and predator traits. The ecological equations for the fixed cost model are defined as

**Fixed Cost Model**

$$\begin{aligned} \frac{dn}{dt} &= \overline{m}_n n = \left( r(1 - \frac{n}{K}) - \gamma e^{(y-x)} \frac{p}{\rho + n} - \alpha x \right) n \\ \frac{dp}{dt} &= \overline{m}_p p = \left( \frac{\beta \gamma e^{(y-x)} n}{\rho + N} - (\delta + \mu y^2) \right) p. \end{aligned} \tag{1.1}$$

In the prey density equation, $r$ is the growth rate of the population in the absence of predation, $K$ is the carrying capacity, $\gamma$ represents the grazing rate of the predator on the prey, $\rho$ is the half-saturation constant of the predator, and $\alpha$ is a parameter which represents the cost of prey defense. In the predator equation, $\beta$ is the

conversion coefficient (how efficiently predators turn prey eaten into offspring), $\delta$ is the natural mortality of predators in the absence of prey, and $\mu$ represents the cost of predator counter-defense.

Evolution is included in the functional response term of the prey equation by scaling the grazing rate by $e^{(y-x)}$. The probability of successful attack by the predator then depends on the relative investment of the prey in defense and the predator in counter-defense. This in turn implies that the birth rate of the predator is directly related to both traits. The probability of successful attack is defined as an exponential equation so that for $x > y$, $e^{(y-x)} > 0$. This ensures that predation always has a negative impact on prey density regardless of the relative contributions to prey defense and predator counter-defense within the populations.

In equation 1.1, we define a linear trade-off curve for the prey, $\alpha x$, where $x$ is the mean trait value as a function of time. For the predator trade-off, counter-defense is a quadratic term, $\mu y^2$, with $y$ representing the mean trait value for the predator. We have chosen to define the predator trade-off as a quadratic so that the predator always invests in a counter-defense regardless of the cost. It is more reasonable however to assume that the prey give up on defense if the cost is too high in favor of increased reproduction so that they do not go extinct in the presence of predation. Defining the prey trade-off as linear ensures that this is the case.

The only difference in the population equations for the variable cost model, is that cost is density-dependent and varies directly proportional to prey density, $n$. The trade-off for prey defense is now defined as $\alpha n x$ and the prey density equation is as follows:

**Variable Cost Model**

$$\frac{dn}{dt} = \overline{m}_n n = \left( r(1 - \frac{n}{K}) - \gamma e^{(y-x)} \frac{p}{\rho + n} - \alpha n x \right) n \tag{1.2}$$

The predator equation for this model does not change from the fixed cost model.

### 1.3.2 Evolutionary Dynamics

The equations describing changes in mean trait values are defined using a quantitative trait (QT) model (see (32; 2) for further discussion). The relative investment of defense and counter-defense affect the probability of a successful attack when a predator encounters its prey. As such, selection on the prey trait is frequency-independent.

Although many of the major assumptions of quantitative trait models are the same as other types of coevolutionary models such as Adaptive Dynamics or ESS (2; 37)), there are two reasons we have chosen the QT approach. First, most of the traits that describe the ability of a predator to capture its prey are a result of many genes with a small, additive effect (3; 32). Second, we wanted a recipe for maintaining polymorphisms in the population. Under this assumption, a variety of genotypes already exist within the population at low frequencies; this allows selection to move rapidly in any direction. This allows for the possibility that evolution can be quite rapid, as opposed to adaptive dynamics which assumes that mutations are rare and therefore, the rate of evolution is slow.

In equations 1.1 and 1.2, population growth rates for the prey and predator are defined as $\overline{m}_n n$ and $\overline{m}_p p$ respectively. Here, $\overline{m}_n$ and $\overline{m}_p$ represent the Malthusian mean fitness as described by (6). The rate of change of the mean trait value is

described as the gradient of fitness of a rare invader with respect to the mean trait value. The trait dynamics for the fixed cost model are

**Fixed cost - trait dynamics**

$$\begin{aligned} \frac{dx}{dt} &= \frac{\partial \overline{m}_n}{\partial x} = \left( \frac{\gamma e^{y-x} p}{\rho + n} - \alpha \right) V_x \\ \frac{dy}{dt} &= \frac{\partial \overline{m}_p}{\partial y} = \left( \frac{\beta \gamma e^{y-x} n}{\rho + n} - 2\mu y \right) V_y. \end{aligned} \tag{1.3}$$

The terms $V_x$ and $V_y$ represent the additive genetic variance (AGV) for the prey and predator populations respectively. We assume that $V_x = A_x x$ and $V_y = A_y y$, where $A_x$ and $A_y$ are the AGV coefficients. We multiply $A_x$ and $A_y$ by the mean trait values, $x$ and $y$, so that as the trait value goes to zero, so does the amount of genetic variation in the population. Changing the value of $A_x$ and $A_y$ changes the relationship between genetic variation and the mean trait value and affects the rate of evolution (a higher value of $A_x$ and $A_y$ implies a faster rate of evolution).

In the variable cost model, because the trait equations are defined in terms of the population density equations, the prey trait equation will also be different, but the predator trait equation will remain unchanged. The expression for the mean prey trait value over time is as follows:

**Variable cost - trait dynamics**

$$\frac{dx}{dt} = \frac{\partial \overline{m}_n}{\partial x} = \left( \frac{\gamma e^{y-x} p}{\rho + n} - \alpha n \right) V_x. \tag{1.4}$$

## 1.4 Analysis

### 1.4.1 Simplifying the Model

In order to simplify the analysis, the models are non-dimensionalized so that the scaled system contains a minimal number of parameters. Another benefit of non-dimensionalized systems is that they help to illustrate the relative scales of parameters in the model. For instance, in equation 1.5, predator density, $p$, is redefined in terms of the prey carrying capacity, $K$, as well as the efficiency of the predator in turning prey into offspring, $\beta$. (For a general discussion on the benefits of non-dimensionalization see (20).) Letting:

$$N = \frac{n}{K},\ P = \frac{p}{\beta K},\ \tau = rt,\ G = \frac{\beta\gamma}{r},\ a = \frac{\alpha K}{r},\ q = \frac{\rho}{K},\ d = \frac{\delta}{r},\ c = \frac{\mu}{r}, \tag{1.5}$$

the fixed cost model becomes:

$$\begin{aligned}
\dot{N} &= \left(1 - N - \frac{Ge^{y-x}P}{q+N} - ax\right)N \\
\dot{P} &= \left(\frac{Ge^{y-x}N}{q+N} - (d+cy^2)\right)P \\
\dot{x} &= \left(\frac{Ge^{y-x}P}{q+N} - a\right)A_x x \\
\dot{y} &= \left(\frac{Ge^{y-x}N}{q+N} - 2cy\right)A_y y
\end{aligned} \tag{1.6}$$

Table 1.1: Parameter definitions and values for the non-dimensionalized equations. The values for $d$, $q$ and $c$ are fixed for the bifurcation analyses. Different values are chosen for $A_x$ and $A_y$ to test the affect of variations in the rate of evolution.

| Parameter | Description | Value |
|---|---|---|
| $a$ | prey defense cost | bifurcation parameter |
| $d$ | predator mortality rate | 0.3 |
| $c$ | predator counter-defense cost | 0.8 |
| $q$ | predator half saturation constant | 0.2 |
| $A_x$ | genetic variation for prey trait | varies |
| $A_y$ | genetic variation for predator trait | varies |
| G | predator grazing rate | bifurcation parameter |

and the variable cost model similarly becomes:

$$\begin{aligned}
\dot{N} &= \left(1 - N - \frac{Ge^{y-x}P}{q+N} - aNx\right) N \\
\dot{P} &= \left(\frac{Ge^{y-x}N}{q+N} - (d + cy^2)\right) P \\
\dot{x} &= \left(\frac{Ge^{y-x}P}{q+N} - aN\right) A_x x \\
\dot{y} &= \left(\frac{Ge^{y-x}N}{q+N} - 2cy\right) A_y y.
\end{aligned} \tag{1.7}$$

Definitions and specific values for the parameters in the non-dimensionalized models can be found in Table 1.1.

Given these simplified equations, the stability of both models can now be compared. The first step is to take the stability analysis of the non-dimensionalized 2-D ecological model to find reasonable parameter values for $d$, $q$, and $G$ that give rise to cycling in the absence of evolution. The same methods for determining equilibria and stability of the system cannot be applied to the 4-D coevolutionary model in part, due to the exponential term in the functional response equation. In order to analyze the full system, we rely on numerical simulations and the equilibrium continuation software, MATCONT (8) to determine the range of parameters $a$, $c$, $A_x$, $A_y$ that give rise to cycling. Predator grazing rate, $G$, (a known bifurca-

tion parameter in the ecological model) and prey trait cost, $a$, are chosen as the bifurcation parameters for stability analysis.

### 1.4.2 Comparing the Dynamics of Evolutionary Models to an Ecological Model

Bifurcation diagrams using prey defense cost, $a$, and predator grazing rate, $G$, reveal interesting differences between the fixed cost and variable cost models (see Figure 1.1). The shaded regions show where cycling can occur. The most immediate and general comparison is that the variable cost model appears to be significantly more stable than either the fixed cost model or the purely ecological Rosenzweig-MacArthur model. This is demonstrated by the fact that the possible range of parameters, $a$ and $G$, that give rise to cycling for the variable cost model are muchsmaller than for either of the other models.

The fixed cost model is qualitatively similar to the Rosenzweig-MacArthur model, both in the range of parameters that generate cycling as well as the type of bifurcation that gives rise to cycling (Figure 1.1). Specifically, for both the fixed cost model and the Rosenzweig-MacArthur model, the system undergoes a super-critical Hopf bifurcation as either $a$ or $G$ are increased. This means that for small enough values of $a$ and $G$ the predator and prey coexist at a stable equilibrium (region **B**). As either parameter increases beyond the bifurcation point, the system loses stability and enters a stable limit cycle oscillation about the former stable equilibrium point (region **C**) (35).

The variable cost model also undergoes a Hopf Bifurcation which gives rise to cycling. In this case however, the system undergoes a sub-critical Hopf. As in a

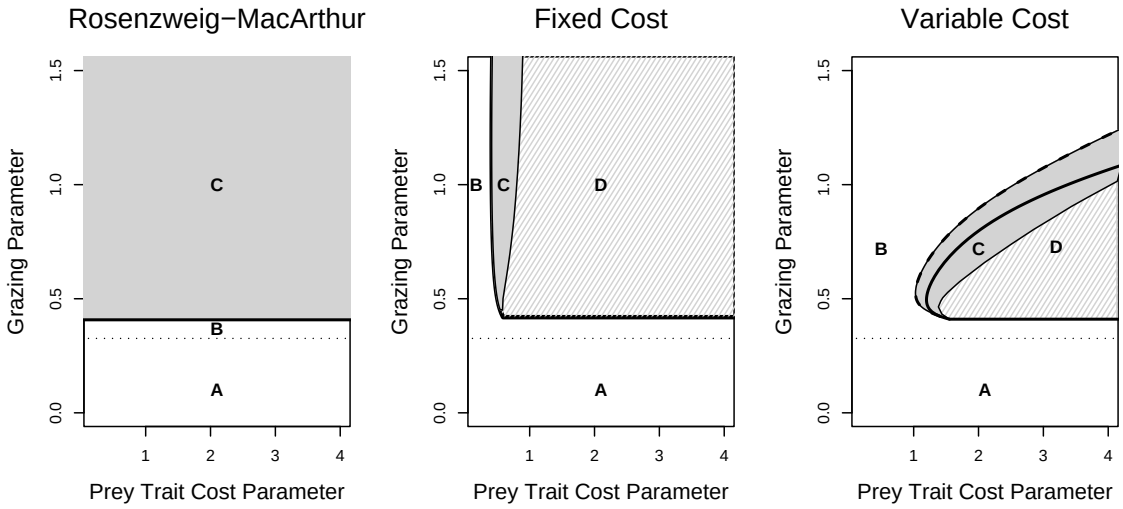


Figure 1.1: Bifurcation diagrams comparing dynamics for the Rosenzweig-MacArthur model (i.e. no evolution) to the Fixed Cost and Variable Cost models. In region **A**, one or both of the populations go extinct, region **B** represents stable coexistence and for the shaded regions **C** and **D** cycling occurs. In the case of the evolutionary models, there are two types of cycling behavior: in region **C** everything cycles (populations and traits); in region **D**, $x \to 0$ and everything else cycles. For the variable cost model, the Hopf curve is marked by a solid line and the curve of Saddle Node of Limit Cycles (SNLC) is denoted by a dashed black line. Between these two lines, the system is bistable (see text for further explanation).

super-critical Hopf, just below the Hopf curve, the stability of the interior fixed point switches and is now stable. What is different about a sub-critical Hopf is that, for a small range of $a$ values near the Hopf curve, the stable fixed point is still surrounded by a stable limit cycle. Furthermore, between the stable fixed point and the stable limit cycle, there exists an unstable limit cycle. Under these conditions, whether the system exhibits cycling or stable co-existence depends on the value of the initial conditions. This is what as known as bistable behavior of the system. The existence of a region of bistability implies that the actual region of cycling can be larger than what is demarcated by the Hopf curve.

Continuing to decrease the value of $a$ causes the system to cross a curve of saddle node of limit cycles (SNLC). This represents a point in parameter space where the

unstable limit cycle and the stable limit cycle collide and only the stable fixed point remains. The solid black line in the bifurcation diagram for the variable cost model represents the curve of Hopf points. The dashed line represents the SNLC curve. In between these two lines is the region of bistability.

Traditionally when oscillatory behavior of a predator-prey system is examined, the emergence of cycling in this 2-D system refers to cycling of the predator and prey densities. Because we are modeling a four dimensional system, what is meant by cycling needs to be more explicitly defined. Here, in the region that cycling exists, predator and prey population cycles persist for all parameter values. The trait dynamics however are more complicated. The predator trait cycles wherever the population dynamics are cycling. The prey, however, will only invest in defense within a small range of $a$ values. Specifically, if the cost for the trait becomes too high, then the prey essentially "give up" on defense in exchange for a higher fecundity rate (i.e. $x \to 0$).

It should be noted that $x = 0$ does not necessarily imply a complete absence of a trait. For example if algae have a defense of increased cell wall thickness in the presence of predation, they obviously do not give up on maintaining a cell wall if the cost is too high. Instead, there is some cell wall thickness that must be maintained for basic survival. In light of this, we can think of the $x = 0$ as being the minimum state that the organism requires for survival. Figure 1.1 shows that, for both models, the range of $a$ and $G$ values for which the prey trait cycles is small relative to the entire region of cycling.

### 1.4.3 Varying the Rate of Evolution

The rate at which evolution is occurring relative to the ecological dynamics can have a dramatic impact on the stability of the interaction (39; 16; 38). Changing the value of the additive genetic variance coefficients $(A_x, A_y)$ is one way to affect the rate at which the two species evolve. The larger the values of these coefficients are, the faster evolution is able to occur. Larger genetic variance coefficients correspond to faster evolution. It does not follow however that setting $A_x = A_y$ will make the speed of evolution in both populations equivalent. For the rate of evolution to be equal the additive genetic variance ($A_x x$ and $A_y y$) would have to be equal.

#### Perturbation Analysis

One way to examine how fast the evolution of each trait is occurring in our system relative to the ecological dynamics is by looking at the rapidity with which the trait dynamics track back to their original state after some small perturbation, $\epsilon$ (see Figure 1.2). To perform this analysis, we test different values of $A_x$ and $A_y$ and observe the dynamics of the perturbed system. The first step is to run simulations on the 4-D coevolutionary system with parameter values that give rise to cycling for both the population and the trait dynamics. Simulations are run for many time steps until stable cycles are reached. A point $(N, P, x, y)$ on this stable periodic orbit is then chosen as the initial condition for a new 6-D perturbed system. Specifically, the 4-D evolutionary model is expanded to include two extra state variables, $\tilde{x}$ and $\tilde{y}$ which represent the perturbed mean trait values. The

initial conditions for the perturbed variables, $\tilde{x}$ and $\tilde{y}$, are set as:

$$\tilde{x} = x + \epsilon x, \qquad \tilde{y} = y + \epsilon y, \tag{1.8}$$

where $\epsilon$ is some small constant ($\epsilon = 0.25$). This new 6-D system of ODEs can be solved for each chosen set of $A_x$ and $A_y$ to determine the rate that evolution is occurring for each trait. The longer it takes for the perturbed traits to track back to their original values of $x$ and $y$, the slower evolution is occurring for that trait.

Figure 1.2 shows the results of the perturbation analysis for the variable cost model. The left column shows the coevolutionary dynamics for the 4-D system at three different levels of the parameters $A_x$ and $A_y$ (0.2, 0.5, 2). The middle column looks at how the perturbed traits track back to their original state on the limit cycle after some small perturbation, $\epsilon$. The last column shows the change in relative traits over time,

$$r_x = \log 10|\frac{x - \tilde{x}}{x}|, \; r_y = \log 10|\frac{y - \tilde{y}}{y}|. \tag{1.9}$$

The steeper the slope of $r_x$ and $r_y$, the faster evolution is occurring. Columns 2 and 3 of Figure 1.2 demonstrate that the predator trait tracks back to its original state faster than the prey trait for all three values of $A_x$ and $A_y$ (0.2, 0.5, 2). As a result, we define the speed of evolution based on how fast the prey are evolving. For the variable cost model, we refer to each of the three levels tested as slow ($A_x = A_y = 0.2$), intermediate ($A_x = A_y = 0.5$) and fast ($A_x = A_y = 2$) evolution.

### Bifurcation Analysis

An interesting pattern begins to emerges when comparing the variable vs. fixed models for different speeds of evolution. In the variable cost model, the effect of

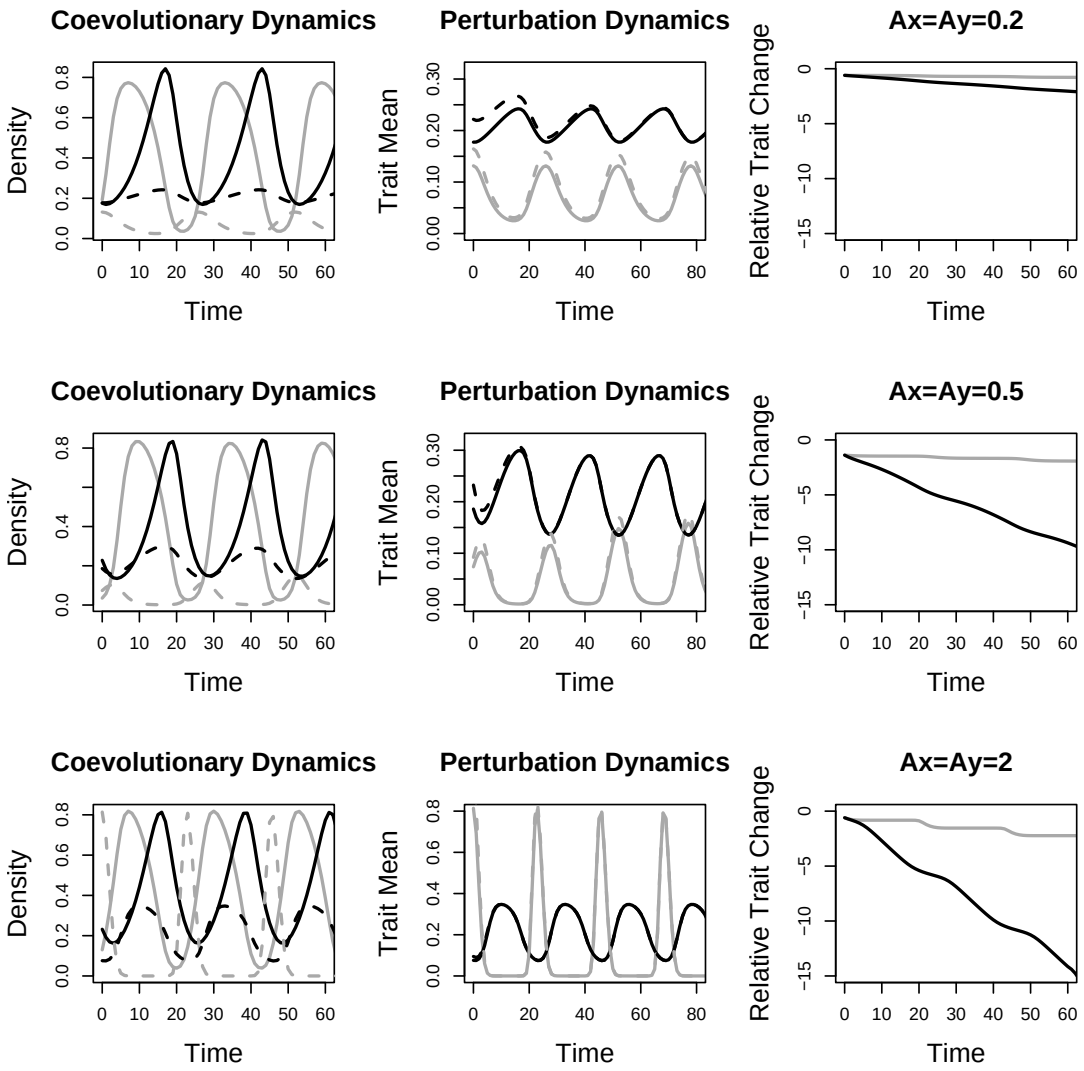


Figure 1.2: Perturbation analysis for the variable cost model for three different levels of $A_x$ and $A_y$ (0.2, 0.5, 2). In all panels, prey dynamics are represented by a gray line and predator dynamics by a black line. [column 1] Cycling dynamics of the 4-D system for 3 different levels of $A_x$ and $A_y$ (0.2, 0.5, 2). The prey and predator densities are shown as solid lines and the trait values as dashed lines. [column 2] Unperturbed traits, $x$ and $y$ (solid lines) and their perturbed counterparts $\tilde{x}$ and $\tilde{y}$ (dashed lines). All other parameters are set constant to the following values: $a = 1.3, d = 0.3, c = 0.8, q = 0.2, G = 0.5$. [column 3] Relative change in each trait value: log10(—original trait  perturbed trait—/original trait). The steeper the slope of each line, the faster evolution is occurring. Note that the axes differs between panels.

increasing the speed of evolution is non-monotonic (see Figure 1.3). For fast evolution ($A_x = A_y = 2$), the region of cycling is very small (i.e., system is stable). As evolution is slowed down, ($A_x = A_y = 0.5$), stability initially decreases up to a point (i.e. the cycling region increases). For $A_x = A_y = 0.2$, the cycling region once again shrinks. For values of $A_x < 0.2$, the prey trait never cycles (i.e. prey trait $x \to 0$ before the Hopf bifurcation occurs. As a result, we do not look at bifurcation diagrams for the variable cost model for $A_x < 0.2$. However, in numerical simulations performed for very small values of $A_x$ and $A_y$ (i.e. $A_x = A_y = 0.01$), it can be shown (results not included here) that the system is increasingly stabilized by decreasing the speed of evolution. Unlike the variable cost model, for the fixed cost model, as evolution slows down, the region of cycling increases monotonically (see Figure 1.4). In other words, the system becomes increasingly less stable as evolution is slowed down. In fact, as $A_x, A_y \to 0$, the range of parameters that give rise to cycling in the fixed cost model approaches that of the Rosenzweig-MacArthur model. It should be noted that the axes are on different scales in Figures 1.3 and 1.4 In addition, the region where one or both species go extinct (see Figure 1.1) has not been drawn in these two figures. The purpose of this is to highlight only the regions of co-existence and in particular, to focus in on how the cycling regions change as $A_x$ and $A_y$ are varied within each model.

### 1.4.4 Comparing Different Rates of Predator-Prey Evolution

The dynamics of both systems are also investigated for the cases where one species is evolving fast or slow relative to the other. The motivation for this is to separate out the relative contribution that prey and predator evolution make to

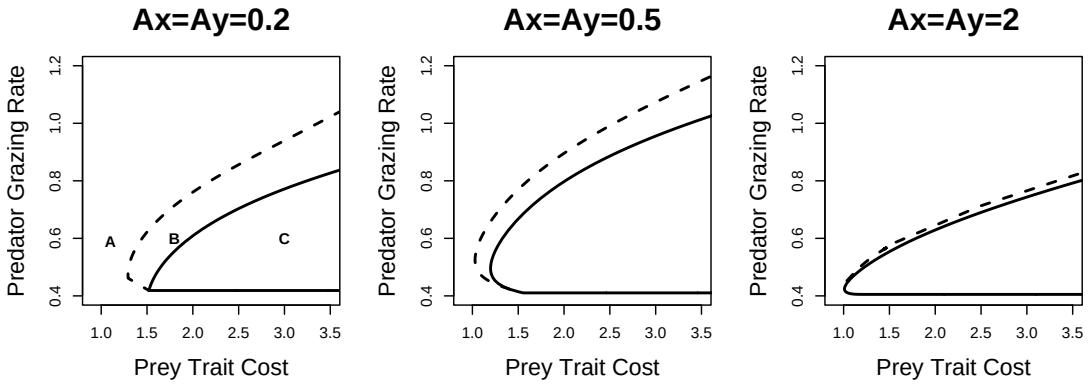


Figure 1.3: Bifurcation diagram for variable cost model showing the cycling region as $A_x$ and $A_y$ are increased from a slow rate of evolution ($A_x = A_y = 0.2$), to an intermediate rate ($A_x = A_y = 0.5$), to a fast rate of evolution ($A_x = A_y = 2$). In region **A** there is stable coexistence of both population and trait dynamics. In region **B**, everything either cycles or there is stable coexistence depending on initial conditions (i.e. bistable region). In region **C**, the prey trait $x \to 0$ while predator trait and population dynamics continue to cycle. The Hopf curve is marked by a solid line and the curve of Saddle Node of Limit Cycles (SNLC) is denoted by the dashed black line. We do not show here the region where one or both populations go extinct. Note that the x- and y-axis do not start at zero to highlight the differences in cycling region in each panel.

the dynamics of the system. Abrams & Matsuda (1997) for example, showed that differences in the time scale between the density of the predator and vulnerability of the prey can lead to destabilization of the interaction (3). In our system, the following cases were analyzed: fast evolving predator and prey, slow evolving predator and prey, fast evolving predator - slow evolving prey, and finally, slow evolving predator - fast evolving prey. In all four cases, we set the additive genetic variance terms to 0.5 when considering fast evolution and to 0.2 when considering slow evolution.

For the fixed cost model, when prey evolve slowly, the system is less stable. The least stable case is when the prey are evolving slowly relative to predator evolution. For the variable cost model, the range of cycling also seems to depend on the rate

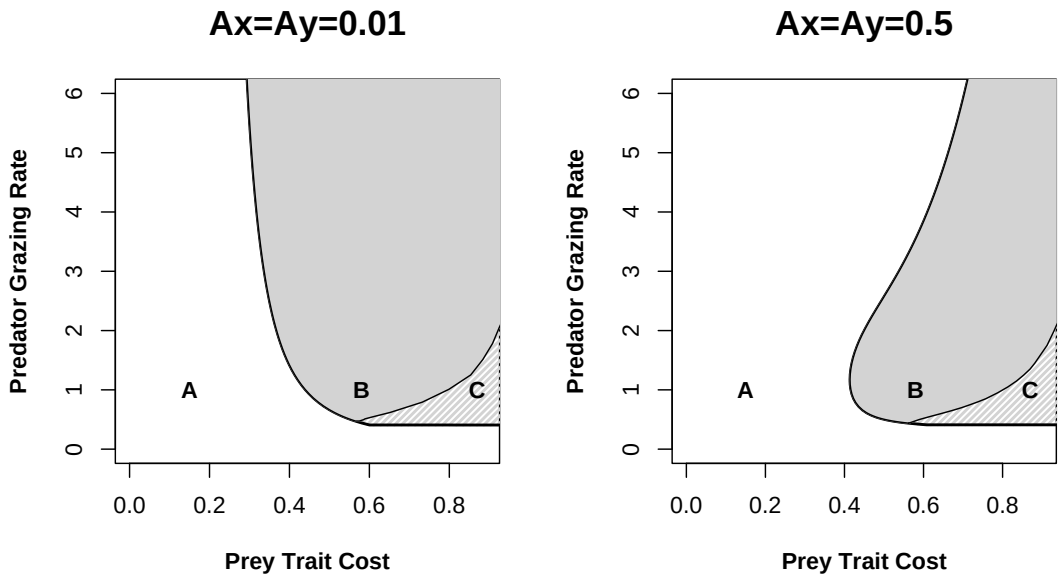


Figure 1.4: Bifurcation diagram for the fixed cost model showing the cycling region as $A_x$ and $A_y$ are increased from a slow rate of evolution ($A_x = A_y = 0.01$) to fast evolution ($A_x = A_y = 0.5$). In region **A** there is stable coexistence of both population and trait dynamics. In region **B**, everything cycles. In region **C**, the prey trait $x \to 0$ while predator trait and population dynamics continue to cycle.

of evolution of the prey. However, in this case a slower rate of prey evolution leads to an increase in stability of the system. The smallest region of cycling occurs for the fast predator - slow prey system and the largest range of cycling occurs for the slow predator - fast prey system (Figure 1.6). A second point to note is that, as prey evolution slows, the region of prey trait cycling is much smaller than when the trait evolves quickly. In fact, in each of the two systems with slow evolving prey, the trait is lost before the Hopf bifurcation is even reached so that prey cycling only occurs in the region of bistability.

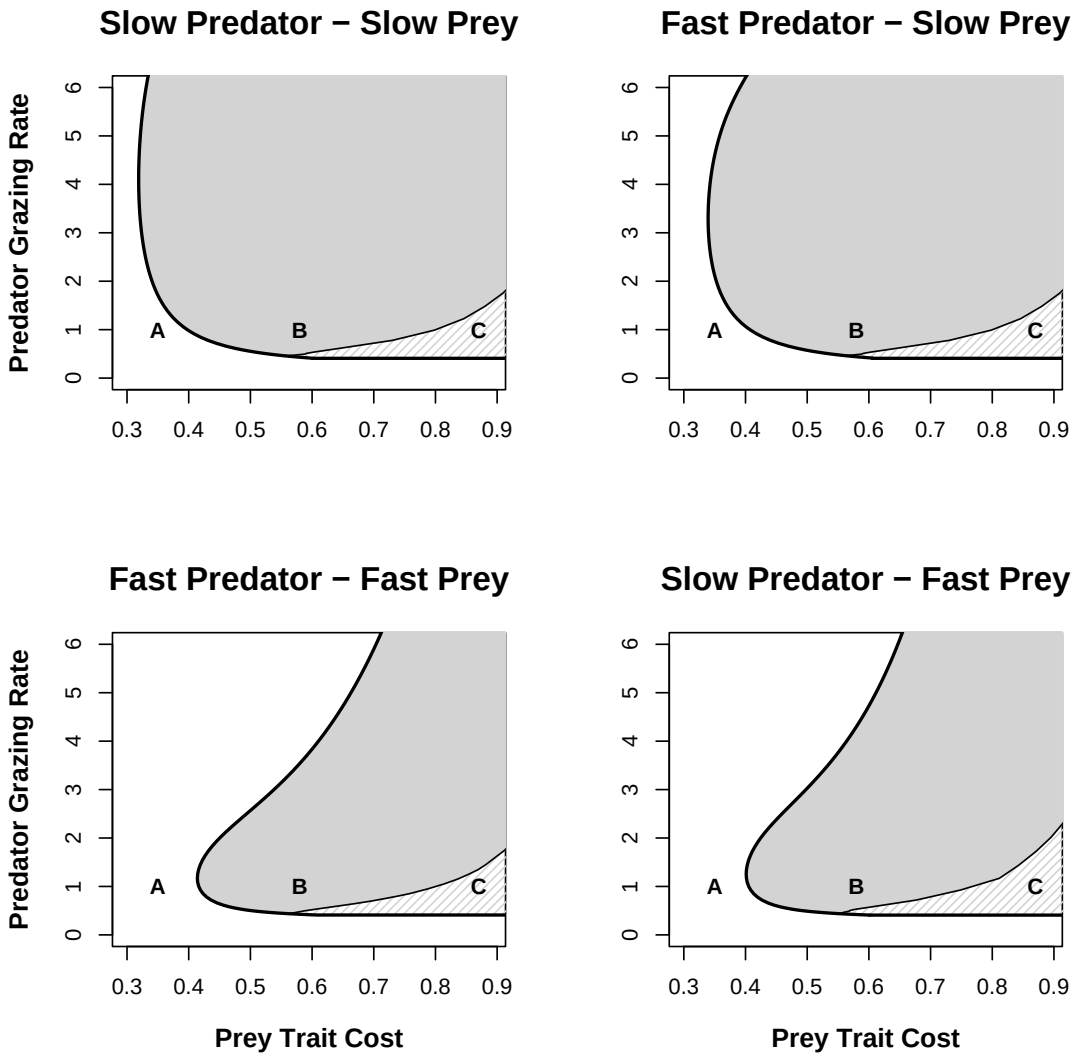


Figure 1.5: Bifurcation diagram for the fixed cost model showing the dynamics when prey are evolving fast or slow relative to the speed of predator evolution. In this case, $A_x = A_y = 0.2$ represents slow evolution and $A_x = A_y = 0.5$ represents fast evolution. (**A**=stable coexistence, **B**=everything cycles and **C**=prey trait $x \to 0$ while predator trait and population dynamics continue to cycle.)

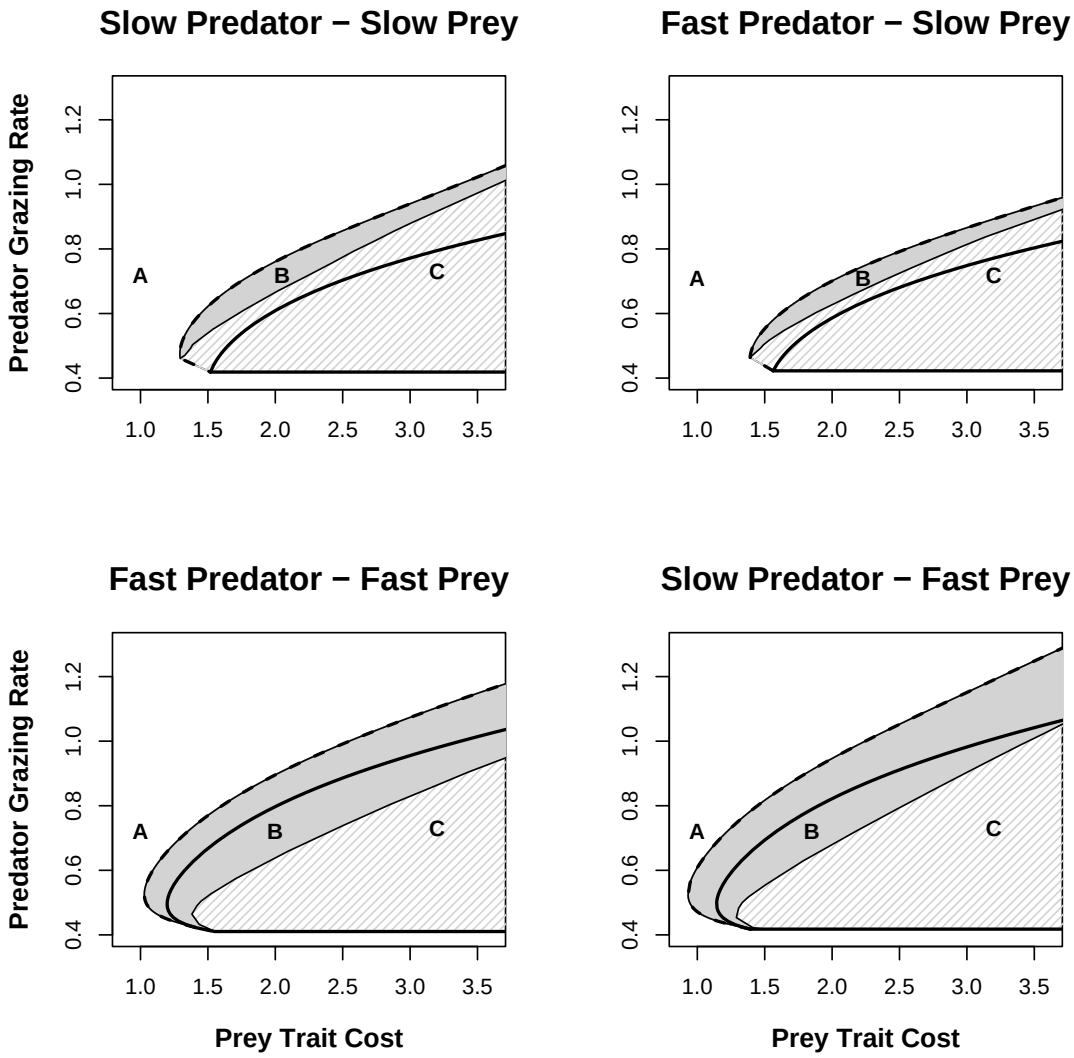


Figure 1.6: Bifurcation diagram for the variable cost model showing the dynamics when prey are evolving fast or slow relative to the speed of predator evolution. $A_x = A_y = 0.2$ represents slow evolution and $A_x = A_y = 0.5$ represents fast evolution. (**A**=stable coexistence, **B**=everything cycles and **C**=prey trait $x \to 0$ while predator trait and population dynamics continue to cycle.)

### 1.4.5 Investigating Criteria for Stability Through Equilibria Comparison

Thus far, we have provided a detailed look at the stability of the system through bifurcation analyses. This was done for a range of $a$ and $G$ values as well as for a small subset of predator and prey additive genetic variance. From this initial analysis, our results indicate that the variable cost model is more stable than the fixed cost model. The robustness of these results can be checked by comparison of equilibrium stability between both models for the full range of all parameters in the system.

For ease of analysis we use a 3-dimensional system that includes prey evolution but no predator evolution. We do this, in part, because our analysis in sections 1.4.3 and 1.4.4 indicate that prey evolution is more important in driving the dynamics than predator evolution. Furthermore, preliminary bifurcation analysis of this model (results not included here) indicated that it is qualitatively similar to the full coevolutionary system and can therefore be used without loss of generality.

**Fixed cost**

$$\begin{aligned} \dot{N} &= N\left(1 - N - \frac{Ge^{-x}P}{q+N} - ax\right) \\ \dot{P} &= P\left(\frac{Ge^{-x}N}{q+N} - d\right) \\ \dot{x} &= xA_x\left(\frac{Ge^{-x}P}{q+N} - a\right) \end{aligned} \tag{1.10}$$

**Variable cost**

$$\begin{aligned} \dot{N} &= N\left(1 - N - \frac{Ge^{-x}P}{q+N} - axN\right) \\ \dot{P} &= P\left(\frac{Ge^{-x}N}{q+N} - d\right) \\ \dot{x} &= xA_x\left(\frac{Ge^{-x}P}{q+N} - aN\right) \end{aligned} \tag{1.11}$$

To ask whether the variable cost model is more or less stable than the fixed cost model, we have to specify how we "pair up" the models that will be compared. One way is to keep parameters the same in the two models; this is what the bifurcation analyses in MATCONT are doing. Another way of comparing the stability of each system is to keep the equilibrium the same between models. In order to match up the two models for direct equilibrium comparison, the variable cost model must be transformed so that it looks like the fixed cost model. Let $a_v$ refer to the cost parameter in the variable cost model and $a_f$ refer to the cost parameter in the fixed cost model. If the value of $a$ in the variable cost model is set to be $a_v = a_f/\bar{N}$, and no other parameter is changed, then the equilibrium point in the fixed cost model, $(\bar{N}, \bar{P}, \bar{x})$ will be the same equilibrium for the variable cost model.

Once a fixed point has been found, we can derive the Jacobians of each system at that equilibrium point and from these matrices obtain the characteristic polynomial:

$$P(\lambda) = \lambda^3 + a_1\lambda^2 + a_2\lambda + a_3. \tag{1.12}$$

The coefficients of this polynomial can be used to derive the Routh-Hurwitz stability criterion. This criterion determines the range of values for each parameter that maintain stable coexistence of the populations. The stability criterion for a $3 \times 3$ system states that in order for a system to be stable, the following three conditions must all hold:

$$c_1 > 0,\ c_3 > 0,\ c_1c_2 - c_3 > 0, \tag{1.13}$$

where $c_1$, $c_2$, and $c_3$ are the coefficients of 1.12. When any of the above conditions are violated, the system becomes unstable and gives rise to cycling.

The Jacobians of this pair of models is first derived using the untransformed

prey trait cost for each model $a_v$ and $a_f$. We use the general result that for a model of the form $\dot{x}_i = x_i r_i(x_1, x_2, \cdots, x_n)$ the Jacobian entries at a steady state where the $x_i$ are all positive are $J_{i,j} = \bar{x}_i \dfrac{\partial r_i}{\partial x_j}$. For the fixed-cost model, the matrix $R_f$, whose $(i,j)^{th}$ entry is $\dfrac{\partial r_i}{\partial x_j}$, is found to be:

$$R_f = \begin{bmatrix} -1 + \dfrac{Ge^{-x}\bar{P}}{\left(q+\bar{N}\right)^2} & -\dfrac{Ge^{-\bar{x}}}{q+\bar{N}} & \dfrac{Ge^{-\bar{x}}\bar{P}}{q+\bar{N}} - a_f \\ \dfrac{Ge^{-\bar{x}}}{\left(q+\bar{N}\right)^2} & 0 & -\dfrac{Ge^{-\bar{x}}\bar{N}}{q+\bar{N}} \\ -\dfrac{A_x Ge^{-\bar{x}}\bar{P}}{\left(q+\bar{N}\right)^2} & \dfrac{A_x Ge^{-x}}{q+\bar{N}} & -\dfrac{A_x Ge^{-\bar{x}}\bar{P}}{q+\bar{N}} \end{bmatrix}. \tag{1.14}$$

The condition that $\dot{x} = 0$ at steady state, namely $\frac{Ge^{-\bar{x}}\bar{P}}{q+\bar{N}} = a_f$, implies that the $(1,3)$ entry of $R_f$ equals 0. The corresponding results for the variable-cost model are:

$$R_v = \begin{bmatrix} -1 + \dfrac{Ge^{-\bar{x}}\bar{P}}{\left(q+\bar{N}\right)^2} - a_v\bar{x} & -\dfrac{Ge^{-\bar{x}}}{q+\bar{N}} & \dfrac{Ge^{-\bar{x}}\bar{P}}{q+\bar{N}} - a_v\bar{N} \\ \dfrac{Ge^{-\bar{x}}}{\left(q+\bar{N}\right)^2} & 0 & -\dfrac{Ge^{-\bar{x}}\bar{N}}{q+\bar{N}} \\ -\dfrac{A_x Ge^{-x}P}{(q+N)^2} - A_x a_v & \dfrac{A_x Ge^{-\bar{x}}}{q+\bar{N}} & -\dfrac{A_x Ge^{-\bar{x}}\bar{P}}{q+\bar{N}} \end{bmatrix}. \tag{1.15}$$

The steady state condition $\dot{x} = 0$ for this model implies that the $(1,3)$ entry of $R_v$ equals 0, where $\frac{Ge^{-\bar{x}}\bar{P}}{q+\bar{N}} = a_v\bar{N}$. Therefore we have

$$R_v - R_f = \begin{bmatrix} -a_v\bar{x} & 0 & 0 \\ 0 & 0 & 0 \\ -A_x a_v & 0 & 0 \end{bmatrix}. \tag{1.16}$$

**Simplifying Jacobians**

The Jacobian for the fixed cost model can be simplified using the steady state conditions (omitting the overbars for convenience)

$$\frac{Ge^{-x}N}{q+N} = d, \qquad \frac{Ge^{-x}P}{q+N} = a_f \tag{1.17}$$

from which it follows that $N/P = d/a_f$ and therefore $a_f N = dP$. The result is

$$J_f = \begin{bmatrix} -N + \dfrac{a_f N}{(q+N)} & -d & 0 \\ \dfrac{a_f}{(q+N)} & 0 & -a_f N \\ -\dfrac{a_f A_x x}{(q+N)} & dA_x x/N & -a_f A_x x \end{bmatrix}. \tag{1.18}$$

Equation (1.16) gives the terms (after multiplication by the fixed point for each row) that must be added to $J_f$ to get $J_v$. The steady state conditions for the variable cost model say that

$$\frac{Ge^{-x}N}{q+N} = d, \qquad \frac{Ge^{-x}P}{q+N} = a_v N \tag{1.19}$$

from which it follows that $N^2/P = d/a_v$ and therefore $a_v N^2 = dP$. The result here is

$$J_v = \begin{bmatrix} -N + \dfrac{a_v N^2}{(q+N)} - a_v N x & -d & 0 \\ \dfrac{a_v N}{(q+N)} & 0 & -a_v N^2 \\ -\dfrac{a_v N A_x x}{(q+N)} - a_v A_x x & \dfrac{dA_x x}{N} & -a_v N A_x x \end{bmatrix}. \tag{1.20}$$

Plugging in the transformation that $a_v = a_f/N$ the only difference in the Jacobians is at $J_v(1,1)$ and $J_v(3,1)$, where

$$J_v - J_f = \begin{bmatrix} -a_f \bar{x} & 0 & 0 \\ 0 & 0 & 0 \\ -\dfrac{a_f}{N} A_x x & 0 & 0 \end{bmatrix}. \tag{1.21}$$

The next step is to derive the characteristic equation for $J_f$ and $J_v$ and look at the Routh-Hurwitz coefficients. Using the stability conditions defined in 1.13, we find that $c_1$, $c_2$ and $c_3$ are all larger for the variable cost model than for the fixed cost model. This means that everything hinges on the final criterion, $c_1 c_2 > c_3$. It suffices for our purposes to show that if we take $c_1 c_2 - c_3$ for the variable-cost model, and subtract off the same quantity for the fixed-cost model, we get something positive. If so, it would show that any time the fixed cost model satisfies the 3rd condition, the variable-cost model does too. In other words, if the coefficients were always larger in the variable cost model, than this system would be always less likely to destabilize then the fixed cost model. The difference is found to be $a^2 x/(q+N)$ times a quadratic polynomial in $A_x$,

$$P = X A_x^2 + Y A_x + Z \tag{1.22}$$

with coefficients

$$\begin{aligned} X &= ax^2(q+N) \\ Y &= qaNx^2 + 2qxN + ax^2N^2 + 2xN^2 - dq - dN - 2axN \\ Z &= dq. \end{aligned} \tag{1.23}$$

In 1.23 the constant and quadratic coefficients ($X$ and $Z$) are always positive. From this, it can be concluded that for $A_x$ very small, or for $A_x$ very large, the variable-cost model will be stable whenever the fixed-cost model is stable. At intermediate values of $A_x$, the situation is not yet clear. As $x \to 0$ we have $Z > 0$, $Y < 0$ and $X \to 0$ ($x \to 0$ would generally result from $a$ being large, but the steady state condition $\dot{N} = 0$ implies $ax < 1$). For extremely small values of $x$, 1.22 becomes negative when $A_x \geq 1$, so we might expect to find fixed cost stable while variable cost is unstable. Because an explicit analytical expression can not be found for the fixed point to determine when $Y$ is positive and when it is negative,

numerical studies are employed to determine under what conditions the stability criteria are violated.

### Numerical study

To understand what happens to the stability of both systems for intermediate values of $A_x$, we generate many random parameter sets, each set representing a specific instance of a fixed point. The parameter set generated must meet the condition that all coordinates are positive when plugged into the equilibrium point, $(\bar{N}, \bar{P}, \bar{x})$. This means that the predator and prey must have a coexistence equilibrium if we set $x = 0$, and at that equilibrium there must be selection for $x$ to increase. This means that $\partial\dot{x}/\partial x > 0$, which yields the condition that $\frac{GP}{q+N} - a > 0$ near $x = 0$. By the usual analysis of the Rosenzweig-MacArthur model, the prey steady state is $\bar{N}_0 = dq/(G - d)$ (from the $\dot{P} = 0$ condition). Due to the scaling of the prey and predator density, both $N$ and $P$ range between zero and one. Setting these bounds on the $\bar{N}_0$ equation, with some algebraic manipulation, we get that there is a prey-predator coexistence equilibrium if $G > dq + d$. The condition $\dot{N} = 0$ implies that when $x = 0$, $G\bar{P}_0/(q+\bar{N}_0) = 1-\bar{N}_0$. There is then selection for $x$ to increase if $a < 1-\bar{N}_0 = 1-\frac{dq}{G-d}$. The following restrictions on the parameters now apply:

$$G > dq + d, \qquad a < 1 - \frac{dq}{G - d}. \tag{1.24}$$

To find equilibrium solutions to test the Routh-Hurwitz criterion, an expression for the fixed point ($\bar{N}$, $\bar{P}$, $\bar{x}$) must be defined in terms of the parameters so that a solution can be found for each parameter set generated. Using the second steady state condition in (1.17), and plugging this in to the non-trivial solution of $\dot{N} = 0$,

we obtain

$$1 - \bar{N} - a - a\bar{x} = 0 \tag{1.25}$$

The first condition in (1.17) can be solved for $\bar{N}$ as a function of $\bar{x}$, giving $\bar{N} = \frac{dq}{Ge^{-x} - d}$. Plugging this in to (1.25), yields an expression for $\bar{x}$ which is monotonically decreasing. The roots of this equation are obtained numerically, and from this, $\bar{N}$ can be computed. In a similar fashion, an explicit solution for $\bar{P} = (a/d)\bar{N}$ can also be found.

We now have the equilibrium solution $(\bar{N}, \bar{P}, \bar{x})$ in terms of the parameters, as well as the constraints on those parameters in order for coexistence. The next step is to generate specific instances of the fixed point and then analyze the stability of this equilibrium point using the Routh-Hurwitz condition, $c_1c_2 - c_3$, for each model. These quantities are referred to as $S_f$ and $S_v$, for the fixed and variable cost models respectively. Specifically, many realizations of the stability conditions are generated for each fixed point using parameter values drawn from a random uniform distribution. The range of parameter is restricted to match the conditions for coexistence in (1.24) such that:

$$\begin{aligned} d &\in (0, 1) \\ q &\in (0, 1) \\ G &\in (1.25, 10) \times (dq + d) \\ a &\in (0, amax),\ amax = 1 - \frac{dq}{G - d} \\ A_x &\in (0.5, 15). \end{aligned} \tag{1.26}$$

This is deliberately a very broad range to give a full scope of how each parameter contributes to stability. In the top left panel of Figure 1.7 it can be seen that, for most of the parameter sets generated, the stability condition $c_1c_2 > c_3$, is not violated for either model. A larger positive value of $c_1c_2 - c_3$ implies a lower

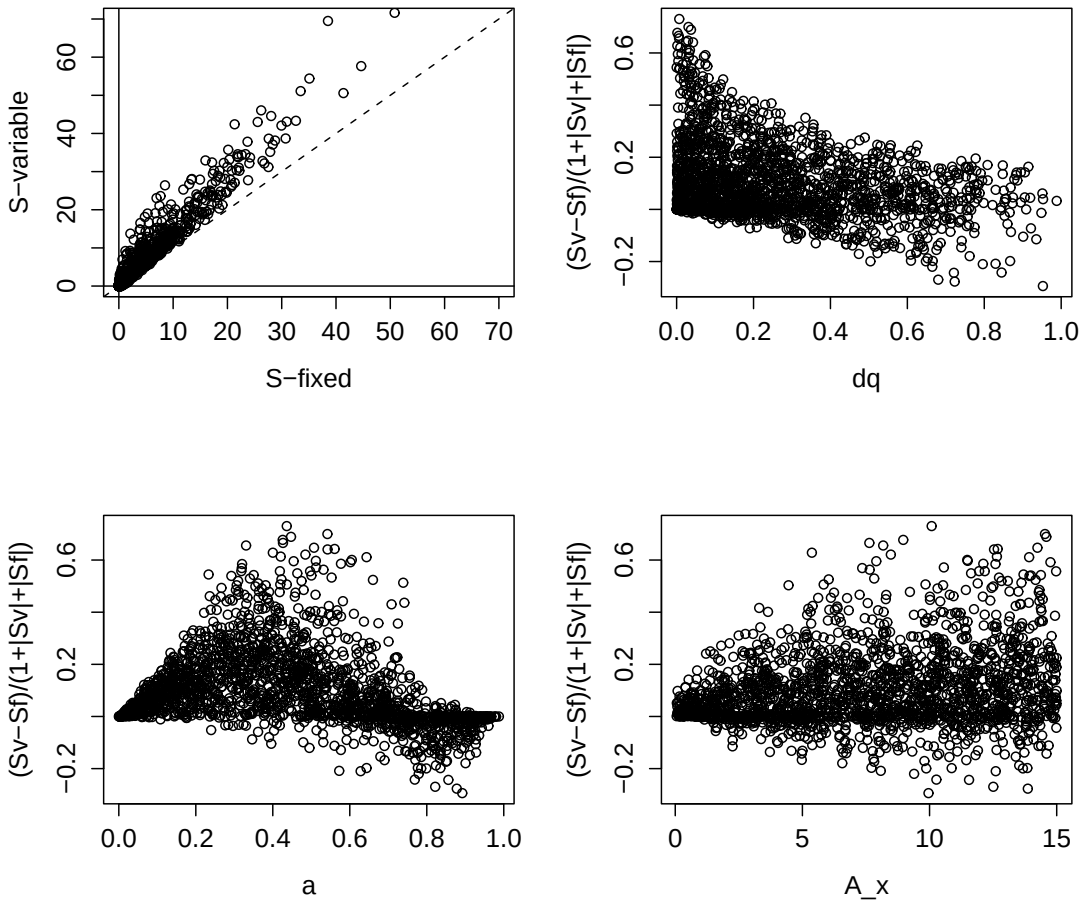


Figure 1.7: Simulation results for Routh-Hurwitz stability criterion with randomly drawn parameter sets. The $y$ axis in all but the top left plot is $(S_v - S_f)/(1+|S_v|+|S_f|)$, which has the same sign as $S_v - S_f$. The top left plot shows the signs of $S_v$ and $S_f$ for each fixed point generated, where a positive value implies stability of the system. The other three panels show what happens to the relative stability of variable vs. fixed cost for relevant parameters: $dq$, $a$, and $A_x$.

likelihood of the system becoming unstable. Interestingly, when comparing the stability criteria for both models, $S_v > S_f$ in 99.7% of the 25000 parameter sets generated. This implies that, even when both systems are stable, in some sense, the variable cost is more stable than the fixed cost model because it it less likely to violate the stability criterion. However, Figure 1.7 also demonstrates that all four logical possibilities can occur and (though rare), that the fixed cost model can sometimes be stable while the variable cost model is unstable ($S_f > 0$ and $S_v < 0$). The other three panels of Figure 1.7 show the relative stability of both models and demonstrates for what parameter values $S_v - S_f < 0$.

Our results indicate that variable cost is more stabilizing than fixed cost over a broader range of all parameter values. To find under what parameter values the reverse is true, we limit our analysis to look only at absolute stability, where $S_v < 0$ and $S_f > 0$. Using a model fitting function (generalized additive model), the condition, $S_v < 0$ and $S_f > 0$, is determined as a function of $A_x$, $a$, $d$ and $q$. These fits can then be used to predict the likelihood of this outcome occurring for different values of each parameter (Figure 1.8). Panel **a** shows that the variable cost model is mostly likely to become destabilized while the fixed cost model remains stable for intermediate rates of prey evolution (at approximately $A_x = 2$). This has been plotted using a large range of $A_x$ values to demonstrate the non-monotonic change in stability of the variable cost model as the speed of evolution is varied.

From the perturbation analysis in section 1.4.3, $A_x = 2$ is already a fast rate of evolution, and probably a more biologically reasonable rate of evolution than $A_x = 15$ which can be equated with an instantaneous rate of evolution. Given this, numerical simulations are run again to determine stability of the fixed points within this reduced range of $A_x$. Panels **b**, **c**, and **d** show the probability of $S_v < 0$

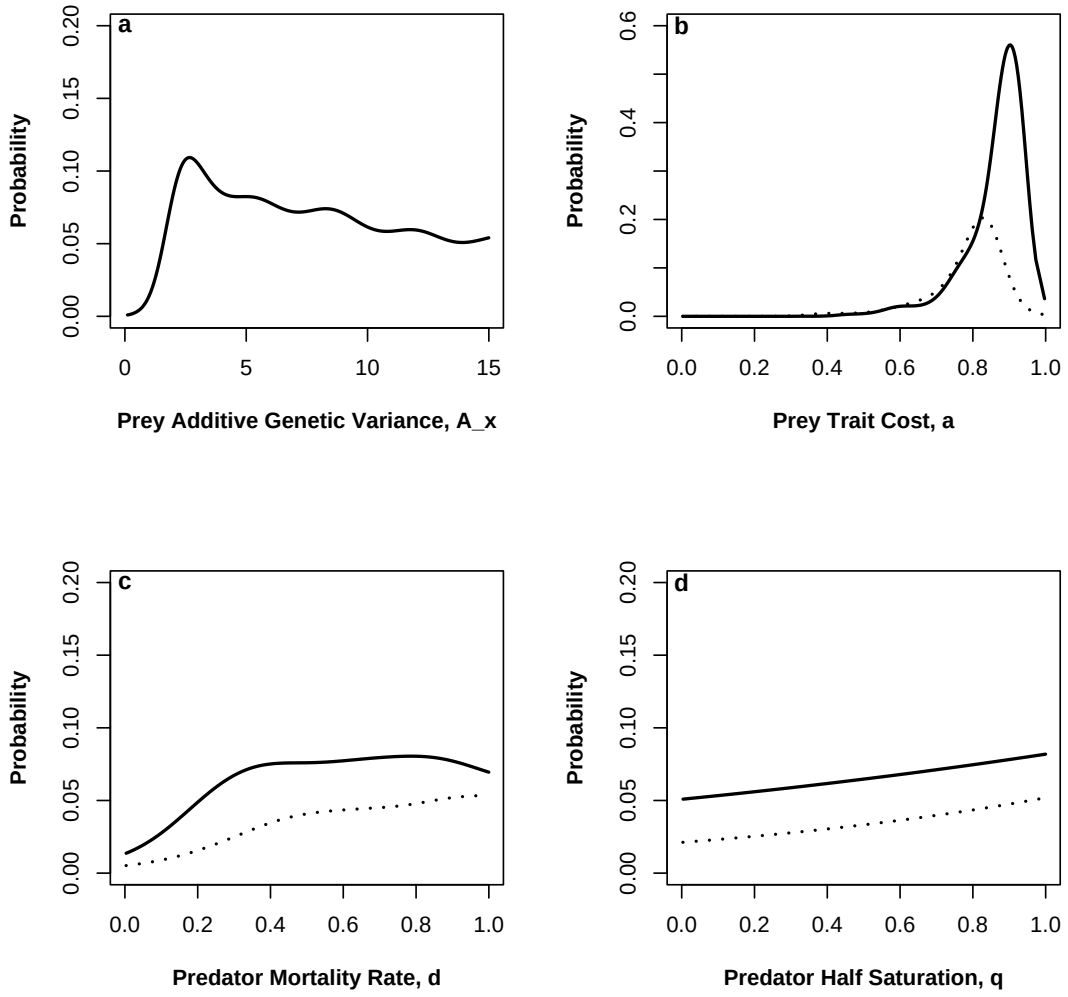


Figure 1.8: Estimated probability that $S_v < 0$ and $S_f > 0$ as a function of $A_x$ (1), $a$ (2), $d$ (3), and $q$ (4), for randomly generated parameter sets. Using the gam function in R, we can obtain a fit for $S_v < 0$ and $S_f > 0$ as a function of each parameter and then predict the likelihood that this outcome will occur as that parameter value is varied. The solid lines in panels **b**, **c** and **d** represent the predicted outcomes based on the full range of $A_x$ values ($A_x \in (0.5, 15)$). The dotted line in each panel shows the outcomes for the restricted range, $A_x \in (0.5, 2)$. See section 1.4.5 in the text for details.

and $S_f > 0$ for parameters $a$, $d$ and $q$. Both the full range of $A_x$ values tested (solid black line), as well as the more biologically realistic subset of $A_x \in (0.5, 2)$ are shown. Reducing the range of $A_x$ values highlights the fact that the probability of the variable cost model becoming unstable while the fixed cost model is stable is relatively small. High cost of defense will destabilize the system up to a point, but is less likely to destabilize the variable cost model at the highest range of $a$ values for which the fixed point exists (panel **b**). As predator mortality, $d$, increases, the probability that, $S_v < 0$ and $S_f > 0$, also increases (panel **c**). Increasing the value of predator half-saturation constant, $q$ has very little affect on the stability of the variable cost model, although higher values are slightly more likely to increase the likelihood that $S_v < 0$ and $S_f > 0$. However, the dotted line in panel **d** shows that the probability of the variable cost model becoming unstable as a function of $q$ shrinks to almost zero when we decrease the range of $A_x$. The parameter that contributes most strongly to the destabilization of the variable cost model is the cost for prey defense, $a$.

### 1.4.6 Understanding the underlying biology

We have employed a variety of numerical methods to analyze the dynamics of both models and our results demonstrate the stabilizing effect that variable cost can have on the dynamics. Here, we discuss why this might be biologically true by looking at what contributes to stability in the variable cost model the prey trade-off curve is redefined. One way to understand the stability of each model is to look at the difference in the Jacobians and to see how each of these terms separately contributes to stability.

The Jacobian of the variable cost model differs from the fixed cost model in

only two entries of the matrix, namely at $J_v(1,1)$ and $J_v(3,1)$ (see equation (1.21)). Biologically, $J_v(1,1)$ represents the impact that a small increase in prey density has on prey growth rate. $J_v(3,1)$ represents the sensitivity of the prey trait to changes in prey density. Recall that, the fitness consequence of the trait is proportional to population size in the variable cost model. Therefore, a change in population size has an effect on the fitness cost of the trait, which is proportional to the mean trait value. In the $J_v(1,1)$ entry, the variable cost model has an extra term, $-a_f\bar{x}$, which reflects the total decrease in fecundity of the prey population based on the mean trait value of the population. In the $J_v(3,1)$ the extra term $-\frac{a_f}{N}A_x x$ can be thought of as the variation in cost due to changes in population size.

What we want to determine is what role each of these extra terms play in the stability of the variable cost model, and under what conditions they lead to the variable cost model becoming less stable than the fixed cost model. We define two additional parameters, $\eta$ and $\epsilon$, where $\eta, \epsilon = 1$. The extra term in $J_v(1,1)$ is multiplied by $\epsilon$ and the extra term in $J_v(3,1)$ by $\eta$. Then, $\eta$ and $\epsilon$ serve simply as markers which allow us to determine what the extra terms in $J_v(1,1)$ and $J_v(3,1)$ contribute to the stability of equation (1.23). From the Routh-Hurwitz stability analysis, the variable cost model is more stable than the fixed cost model whenever equation (1.23) is greater than zero. Repeating the Jacobian analysis of section 1.4.5 with the inclusion of $\eta$ and $\epsilon$, a new expression for $S_v - S_f$ can be obtained. As in 1.22, this polynomial expresses the difference in the Routh-Hurwitz criterion, $c_1c_2 - c_3$, for each model. Adding $\epsilon$ and $\eta$ to $J_v$, the new coefficients are:

$$\begin{aligned} X &= ax^2(q+N)\epsilon \\ Y &= qNax^2\epsilon^2 + 2qxN\epsilon + ax^2N^2\epsilon^2 + 2xN^2\epsilon - dq\eta - dN\eta - 2axN\epsilon \\ Z &= dq\epsilon \end{aligned} \tag{1.27}$$

In the above equation, $\eta$ appears only in the $Y$ coefficient and is always associated with a negative value. This implies that in equation 1.16 the extra term in $J_v(3,1)$ always contributes to the instability of the variable cost model. In other words, a small change in prey density will lead to cycling of the prey trait. The fact that $J_v(3,1)$ always contributes to cycling behavior of the system implies that what makes the variable cost model more stable than the fixed cost model lies entirely in the difference between the two Jacobian matrices at $J_v(1,1)$. Looking at the contribution of $J_v(1,1)$ to the sign of $Y$ (by observing which terms include $\epsilon$), it can be seen that $\epsilon$ is positive in all the terms but one ($-2axN\epsilon$). We can conclude from this that an increase in prey density mostly has a positive (i.e. stabilizing) affect on prey growth rate, but under some conditions can be destabilizing. (Recall that for this analysis we are looking at the equilibrium value of $\bar{N}$, which is defined in terms of all the parameters in our system. This means that all parameters contribute to the destabilizing effect of $-2axN\epsilon$.)

If the extra term in $J_v(1,1)$ were removed so that $J_v(1,1) = J_f(1,1)$, then the variable cost model would always be less stabilizing than the fixed cost for all parameter values. So why exactly does a small change in prey density generally have a stabilizing effect on prey growth rate? At high densities, defense is very costly due to increased prey density. Prey give up very quickly on defense, and as a consequence, they get reduced down to low density by the predator. At the same time, once the defense is lost, there is a lower cost for defense and because density and cost are both low, prey are able to initially grow very quickly. However, as they grow, so does the cost which then acts to drag the population back down. The result is that population cycles tend to get damped out.

## 1.5 Discussion

Our major results are:

- Adding evolution to the ecological predator-prey system stabilizes the interaction.
- There is a trade-off between fecundity and defense which leads prey to "give up" on defense when cost is too high.
- Variable cost of prey defense is more stabilizing than fixed cost except in rare cases.
- The fixed cost model is increasingly more stable as the rate of evolution increases. For variable cost, the system is stabilized by very slow or very fast evolution and less stable for intermediate rates of evolution.
- The effect of relative rate of prey and predator evolution on stability differs between the models. Fast prey evolution stabilizes the fixed cost model, but destabilizes the variable cost model, at least within an intermediate range of prey additive genetic variance.

Our results indicate that evolution can have a stabilizing affect on population dynamics, regardless of how the cost of prey defense is defined. Historically, little thought has been given to the importance of evolutionary change on ecological dynamics. This was largely due to the belief that the evolutionary dynamics occurred on a much slower time scale than the ecology and therefor were irrelevant in controlling the ecological dynamics. There is mounting evidence however, both in models and in empirical studies (3; 22; 38) that evolutionary dynamics can play a large role in the stability of predator-prey interactions. Jones et al. (2009),

for example, found that classic predator-prey cycles in a rotifer-algal chemostat could be suddenly damped out when algae evolved a defense against predation (16). One explanation for the stabilizing effects of evolution is that the energetic cost for investment in a trait can lead to a trade-off between fecundity and defense (4; 18; 40). The existence of trade-offs naturally imposes a constraint on how defended the prey population can become (24).

When we allowed both species to evolve but imposed a trade-off between defense and fecundity our system was more stable relative to the ecological model, regardless of whether prey defense cost was variable or fixed. Yet, how sensitive this cost is to environmental stress (i.e. increased population density) can have a large impact on just how stabilizing evolution is, particularly when evolution is occurring very slowly relative to the ecology. Where the cost of defense is density-independent (fixed cost model) and evolution is slow, there is very little difference in the cycling regime with a model that incorporates no evolution at all. In contrast, the dynamics for density-dependent costs are quite stable for low rates of evolution. Observations of natural systems often do not exhibit cycles as frequently as is predicted by the paradox of enrichment (21; 26; 15; 31). The fact that variable cost of prey defense is so stabilizing might be one explanation for why this is so.

We have seen from both models, that the cost of prey defense can act in self-regulating the prey. The difference between the fixed and variable cost model is how self-regulating the cost of defense is. In the case where cost is variable, so is the amount of self-regulation. An increase in prey density in the model corresponds to a proportional increase in the cost to defend. This ensures that prey do not overshoot their equilibrium, a situation known to give rise to cycling

in the classical predator-prey model. The result is that variable cost regulates the effects of the paradox of enrichment. In contrast, in the fixed cost model when the cost of defense is low, prey are more likely to overshoot their equilibrium as population density increases. This leads to a scenario described by (29) as prey escape. Here, there is a delay before the predator population can respond, which gives rise to population cycling. When cost is high and prey population density is low, predation acts to suppress the prey far below their natural carrying capacity which also can lead to cycles. (25) define as the suppression-stability trade-off. These two examples highlight that mechanisms exist in the fixed cost model both at low and high prey densities that may lead to the continuation of cycles that do not exist in the variable cost model.

We have seen that the sensitivity of defense cost to prey density can be quite important in determining the dynamics of the system. In addition, the relative speed of predator verses prey evolution plays a large role in the stability of the system. However, the rate at which the prey evolve appears to control population dynamics much more strongly than the speed of predator evolution. In general, although predator evolution alone can drive population cycles, it is unlikely to do so (1). The importance of prey evolution to the ecological dynamics in our models was emphasized by the fact that the 3-D which included only prey evolution were qualitatively quite similar to the full 4-D evolutionary models. These results are consistent with a study by (38) which showed that very little generalization about the model was lost through the exclusion of predator evolution. In other words, prey evolution was the driving force for shifts in population dynamics. In addition, their model showed that as the speed of evolution increased, so did stability of the system.

From numerical analysis of the Routh-Hurwitz criterion, we determined that when prey evolve very quickly or very slowly relative to the ecological dynamics, the variable cost model is always more stable than the fixed cost model, but at intermediate rates of prey evolution, variable cost can sometimes be less stable. Other factors that contribute to the variable cost model occasionally becoming unstable while fixed cost remains stable are an increase in the following: prey defense cost, predator mortality rate and predator half-saturation constant (a measure of grazing efficiency). A known result of predator-prey interactions is that an increase in predator grazing efficiency can destabilize an otherwise stable interaction (1). It is somewhat surprising then, that a *less* efficient predator might destabilize an otherwise stable system. However, from Figure 1.8, there is very little increase in the probability that the variable cost model becomes unstable while fixed cost remains stable as the half-saturation constant, $q$ increases. In addition, (1) has shown that a decrease in predator grazing when the prey are abundant can lead to destabilization and this scenario might be possible if the predator is a less efficient grazer. The parameter that is most important in determining the stability of the variable cost model is prey defense cost, $a$. It is not surprising that this is such an important parameter in the variable cost model as it is directly linked to population density. In effect, prey cost serves to hold the prey equilibrium far below the natural prey carrying capacity which has a known destabilizing effect on the interaction.

One argument that has been posed for the creation of eco-evolutionary models to describe predator-prey interactions is that evolution can happen on an ecological time scale and can therefore directly impact the type of dynamics seen in the system (1; 39; 14; 16). This is certainly true in both the fixed and variable cost models when the speed of evolution is fast. However, we would argue that, in

the case where the cost of prey defense is impacted by environmental stress (i.e. variable cost model) considering evolution is important when studying population dynamics. This is true even when the rate of evolution is much slower than the ecological dynamics.

## BIBLIOGRAPHY


[1] P. A. Abrams. The evolution of predator-prey interactions: Theory and evidence. *Annual Review of Ecology and Systematics*, 31:79–105, 2000.

[2] P. A. Abrams. Modelling the adaptive dynamics of traits involved in inter- and intraspecific interactions: An assesment of three methods. *Ecology Letters*, 4:166–175, 2001.

[3] P. A. Abrams and H. Matsuda. Prey adaptation as a cause of predator-prey cycles. *Evolution*, 51:1742–1750, 1997.

[4] E. D. III Brodie and E. D. Jr. Brodie. Costs of exploiting poisonous prey: Evolutionary trade-offs in a predator-prey arms race. *Evolution*, 53:626–631, 1999.

[5] D. O. Conover and S. B. Munch. Sustaining fisheries yields over evolutionary time scales. *Science*, 297:94–96, 2002.

[6] J. F. Crow and M. Kimura. *An introduction to population genetics theory.* Harper and Row, 1970.

[7] R. Dawkins and J. R. Krebs. Arms races within and between species. *Proceedings of the Royal Society London, B*, 205:480–512, 1979.

[8] A. Dhooge, W. Govaerts, and Y. A. Kuznetsov. MATCONT: A Matlab package for numerical bifurcation analysis of odes. *ACM Transactions on Mathematical Software*, 29:141–164, 2003.

[9] U. Dieckmann. Can adaptive dynamics invade? *Trends in Ecology and Evolution*, 12:128–131, 1997.

[10] U. Dieckmann and R. Law. The dynamical theory of coevolution: a derivation from stochastic ecological processes. *Journal of Mathematical Biology*, 34:579–612, 1996.

[11] U. Dieckmann, P. Marrow, and R. Law. Evolutionary cycling in predator-prey interactions: population dynamics and the red queen. *Journal of Theoretical Biology*, 176:91–102, 1995.

[12] M. D. E. Fellowes and J. M. J. Travis. Linking the coevolutionary and population dynamics of host-parasitoid interactions. *Population Ecology*, 42:195–203, 2000.

[13] S. A. H. Geritz, J. A. J. Metz, E. Kisdi, and G. Meszéna. Dynamics of adaptation and evolutionary branching. *Physical Review Letters*, 78:2024–2027, 1997.

[14] N. G. Hairston, S. P. Ellner, M. A. Geber, T. Yoshida, and J. A. Fox. Rapid evolution and the convergence of ecological and evolutionary time. *Ecology Letters*, 8:1114–1127, 2005.

[15] C. X. J. Jensen and L. R. Ginzburg. Paradoxes or theoretical failures? the jury is still out. *Ecological Modelling*, 188:3–14, 2005.

[16] L. E. Jones, L. Becks, S. P. Ellner, N. G. Hairston, T. Yoshida, and G. Fussman. Rapid contemporary evolution and clonal food web dynamics. *Philosophical Transactions of the Royal Society B*, 364:1579–1591, 2009.

[17] L. E. Jones and S. P. Ellner. Evolutionary tradeoff and equilibrium in an aquatic predatorprey system. *Bulletin of Mathematical Biology*, 66:1547–1573, 2004.

[18] A. R. Kraaijeveld and H. C. J. Godfray. Trade-off between parasitoid resistance and larval competitive ability in *Drosophila melanogaster*. *Nature*, 389:278–280, 1997.

[19] A. R. Kraaijeveld, K. A. Hutcheson, E. C. Limentani, and H. C. J. Godfray. Costs of counterdefenses to host resistance in a paristoid *Drosophila*. *Evolution*, 55:1815–1821, 2001.

[20] C. C. Lin and L. A. Segal. *Mathematics applied to deterministic problems in the natural sciences*. MacMillan, New York, 1974.

[21] E. McCauley and W. W. Murdoch. Predator-prey dynamics in environments rich and poor in nutrients. *Nature*, 343:455–457, 1990.

[22] E. McCauley, R. M. Nisbet, W. W. Murdoch, A. M. de Roos, and W. S. C. Gurney. Large amplitude cycles of *Daphnia* and its algal prey in enriched environments. *Nature*, 402:653–656, 1999.

[23] J. A. J. Metz, S. A. H. Geritz, G. Meszna, F. J. A. Jacobs, and J. S. van Heerwaarden. Adaptive dynamics, a geometrical study of the consequences of nearly faithful reproduction. In S. J. van Strien and S. M. Verduyn Lunel, editors, *Stochastic and spatial structures of dynamical systems*, pages 183–231. Elsevier, Amsterdam, 1996.

[24] T. Mitchell-Olds. Pleiotropy causes long-term genetic constraints on life-history evolution in *Brassica rapa*. *Evolution*, 50:1849–1858, 1996.

[25] W. W. Murdoch, C. J. Briggs, and R. M. Nisbet. *Consumer-Resource Dynamics*. Princeton University Press, 2003.

[26] W. W. Murdoch, R. M. Nisbet, E. McCauley, A. M. de Roos, and W. S. C.

Gurney. Plankton abundance and dynamics across nutrient levels: tests of hypotheses. *Ecology*, 79:1339–1356, 1998.

[27] F. Pelletier, T. Clutton-Brock, J. Pemberton, S. Tuljapurkar, and T. Coulson. The evolutionary demography of ecological change: linking trait variation and population growth. *Science*, 315:1934–1937, 2007.

[28] D. N. Reznick, F. H. Shaw, F. H. Rodd, and R. G. Shaw. Evaluation of the rate of evolution in natural populations of guppies (*Poecilia reticulata*). *Science*, 275:1934–1937, 1997.

[29] A. M. De Roos, J. A. J. Metz, E. Evers, and A. Leipoldt. A size-dependent predator-prey interaction: Who pursues whom? *Journal of Mathematical Biology*, 28:609–643, 1990.

[30] M. L. Rosenzweig and R. H. MacArthur. Graphical representation and stability conditions of predator-prey interactions. *American Naturalist*, 97:209–223, 1963.

[31] S. Roy and J. Chattopadhyay. The stability of ecosystems: A brief overview of the paradox of enrichment. *Journal of Biosciences*, 32:421–428, 2007.

[32] I. Saloniemi. A coevolutionary predator-prey model with quantitative characters. *American Naturalist*, 141:880–896, 1993.

[33] A. Sasaki and H. C. J. Godfray. A model for the coevolution of resistance and virulence in coupled host-parasitoid interactions. *Proceedings of the Royal Society of London, B*, 266:455–463, 1999.

[34] K. W. Shertzer, S. P. Ellner, G. F. Fussmann, and N. G. Hairston. Predator-prey cycles in an aquatic microcosm: testing hypotheses of mechanism. *Journal of Animal Ecology*, 71:802–815, 2002.

[35] S. H. Strogatz. *Nonlinear dynamics and chaos: With Applications To Physics, Biology, Chemistry And Engineering.* Westview Press, 1994.

[36] L. Van Valen. A new evolutionary law. *Evolutionary Theory*, 1:1–30, 1973.

[37] D. Waxman and S. Gavrilets. Issues of terminology, gradient dynamics and the ease of sympatric speciation in adaptive dynamics. *Journal of Evolutionary Biology*, 18:1214–1219, 2005.

[38] A. Yamauchi and N. Yamamura. Effects of defense evolution and diet choice on population dynamics in a one-predator-two-prey system. *Ecology*, 86:2513–2524, 2005.

[39] T. Yoshida, S. P. Ellner, and N. G. Hairston. Evolutionary trade-off between defence against grazing and competitive ability in a simple unicellular alga, *Chlorella vulgaris*. *Proceedings of the Royal Society of London, B*, 271:1947–1953, 2004.

[40] T. Yoshida, L. E. Jones, S. P. Ellner, G. F. Fussmann, and N. G. Hairston. Rapid evolution drives ecological dynamics in a predatorprey system. *Nature*, 424:303–306, 2003.

[41] T. Yoshida, S. P. Ellner L. E. Jones, B. J. M. Bohannan, R. E. Lenski, and N. G. Hairston. Cryptic population dynamics: rapid evolution masks trophic interactions. *PLoS Biology*, 5:1868–1879, 2007.

CHAPTER 2

# TOP-DOWN VS. BOTTOM-UP CONTROL OF *CALANUS FINMARCHICUS* IN THE GULF OF MAINE

## 2.1 Abstract

During the 1990s the Gulf of Maine (GOM) underwent an ecosystem regime shift associated with an increase in freshwater inputs. This freshening has been linked to increased phytoplankton abundance, which in turn positively affected the growth of zooplankton and, consequently, many pelagic fish populations. *Calanus finmarchicus* is one of the most abundant species of zooplankton in the GOM and so is an important prey source for many species higher up the food chain such as herring and the North Atlantic right whale. While reproduction for *C. finmarchicus* was high during this period, abundance of the later stages of the surface population was paradoxically low. Adult herring preferentially feed on the later copepodid stages; it is therefore possible that increased herring presence exerted top-down control on *C. finmarchicus*. An alternative hypothesis is that the changes in phytoplankton abundance during the 1990s impacted recruitment of *C. finmarchicus* into the later stages. Specifically, phytoplankton variability may impact whether *C. finmarchicus* remain at the surface to reproduce or enter into a resting state until the following year, emerging to take advantage of the spring bloom. Using three simple differential equation models, we examined the interplay of top-down verses bottom-up processes on the observed changes in seasonal patterns of surface populations of late-stage *C. finmarchicus*. Two of the models defined recruitment into late-stage *C. finmarchicus* as a function of available phytoplankton, where development into the later-stages was described as either a

decreasing or increasing function of food. The third model assumed that a fixed fraction enter into the later-stages regardless of available food. For each model, we examined three different cases to test the importance of top-down vs. bottom-up processes: both food availability and fish abundance increased in the 1990s; food abundance stayed the same but fish increased; fish abundance stayed the same but food increased. Time series data for *C. finmarchicus* and for phytoplankton abundance were obtained from the GOM Continuous Plankton Recorder survey which has been collected since 1969. Other reasonable parameter values were obtained directly from the literature or through maximum likelihood estimates. The goodness-of-fit of each model was quantified using the Akaike Informational Criterion (AIC). The best fit to the data was the model which described development into the later stages as a decreasing function of food and incorporated changes in both herring and phytoplankton abundances.

## 2.2 Introduction

In the period between 1992 and 2002 in the Gulf of Maine (GOM), water salinity declined across the Northwest Atlantic (41). Freshining was associated with an increase in phytoplankton abundance particularly during autumn (23). This in turn, led to increased abundance of most zooplankton species (48), including early stages of *C. finmarchicus*. *C. finmarchicus* is particularly abundant in the North Atlantic, comprising more than half of the total zooplankton biomass (49; 31). While the abundance of early *C. finmarchicus* stages was high throughout the 1990s, recruitment into the later stages was paradoxically low (48). The decline of the later stages has been studied extensively in the last decade, in part because *C. finmarchicus* is an important food source for a number of planktivorous species including cod, herring (33; 14) and the endangered North Atlantic right whale *Eubalena glacialis* (22; 5; 54).

A number of theories have been proposed to explain this decrease in late-stage *C. finmarchicus*. Some researchers have suggested that increased abundance of pelagic fish species in the 1990s led to a top-down control on *C. finmarchicus* (17; 18; 4). This might be particularly true of herring which preferentially feed on late-stage *C. finmarchicus* (7; 14). An alternative theory is that changes in phytoplankton abundance, which were tied to increased water freshening, affected recruitment of *C. finmarchicus* into adulthood (29; 31). Specifically, whether *C. finmarchicus* transition into diapause (i.e. resting state) in deeper water at the end of the early copepodite stages or instead remain at the surface to moult into adulthood and reproduce has been linked to the amount of available phytoplankton.

For this study, we will focus on the late-stage surface populations *C. finmarchi-*

*cus*. We incorporate both predation by herring and seasonal variations in phytoplankton abundance to understand the role each might have played in the decreased abundance of late stage *C. finmarchicus*. Our main questions are: If the 1990s saw an increase in fresh water and thereby an increase in *C. finmarchicus* reproduction, why was there a decrease in recruitment into the later age classes? Can this decrease be explained by seasonal changes in food availability alone or is the inclusion of increased herring presence needed in order to explain the patterns of abundance observed in the 1990s?

We propose to answer these questions through a series of differential equation models describing changes in abundance of late-stage *C. finmarchicus*. Herring and phytoplankton abundances are included in the models as seasonally varying forcing terms. We examine three models based on different hypotheses about the mechanism controlling recruitment: the probability of entering into the non-diapausing population is a decreasing function of available food; the probability of entering into these stages is an increasing function of food; a fixed fraction enter into the later stages independent of phytoplankton abundance. For each model, we consider three cases describing the relative roles of top-down and bottom-up process: both phytoplankton and herring abundances were higher than normal between the 1980s and the 1990s; only herring abundance increased in the 1990s, while food abundance remained the same (averaged across decades); only phytoplankton increased in the 1990s while herring remained the same. Throughout the paper, we refer to each combination of "model/case" as a "scenario". Goodness-of-fit of scenarios is determined through the use of the Akaike Information Criterion (1). Our results indicate that the best fit to the data is the scenario which assumes that transition into the late-stage non-diapause class is a decreasing function of food and that both phytoplankton and herring abundance were higher in the 1990s.

## 2.3 Background and Hypotheses

### 2.3.1 Observed climate and zooplankton data

The NW Atlantic experienced a general water freshening throughout the 1990s from the Labrador Sea to the mid-Atlantic bight (23). This colder, less saline water was, in part, a result of changes in atmospheric pressure in the Arctic which brought on circulation shifts that moved freshwater down into the region. An observed reduction in the amplitude of the annual temperature cycle in late winter/early spring throughout this decade implies that winter mixing was decreased (41). Increased stratification in turn led to an unusually high phytoplankton and zooplankton abundance in autumn (15) (Figures 2.1 and 2.2). This shift in abundance was seen throughout the entire annual cycle during the 1990s. Smaller species of zooplankton such as *Centropages typicus* and *Oithona* spp., which predominantly rely on the fall bloom for growth, exhibited a dramatic jump in abundance of almost an order of magnitude from their average density in the 1980s (panels **A, B** of Figure 2.2). We refer to these species throughout the remainder of the paper simply as *Centropages* and *Oithona*. Early stages of *C. finmarchicus*, which are generally more of a spring-dominated species, nonetheless also demonstrated an increase in abundance from their levels in the previous decade (panel **C**) (48). However the later stages of *C. finmarchicus* exhibited a simultaneous decrease in seasonal abundance (panel **D**). Statistical analysis for differences in mean seasonal abundances between decades for phytoplankton, zooplankton spp., and sea surface temperature can be found in Table 2.1.

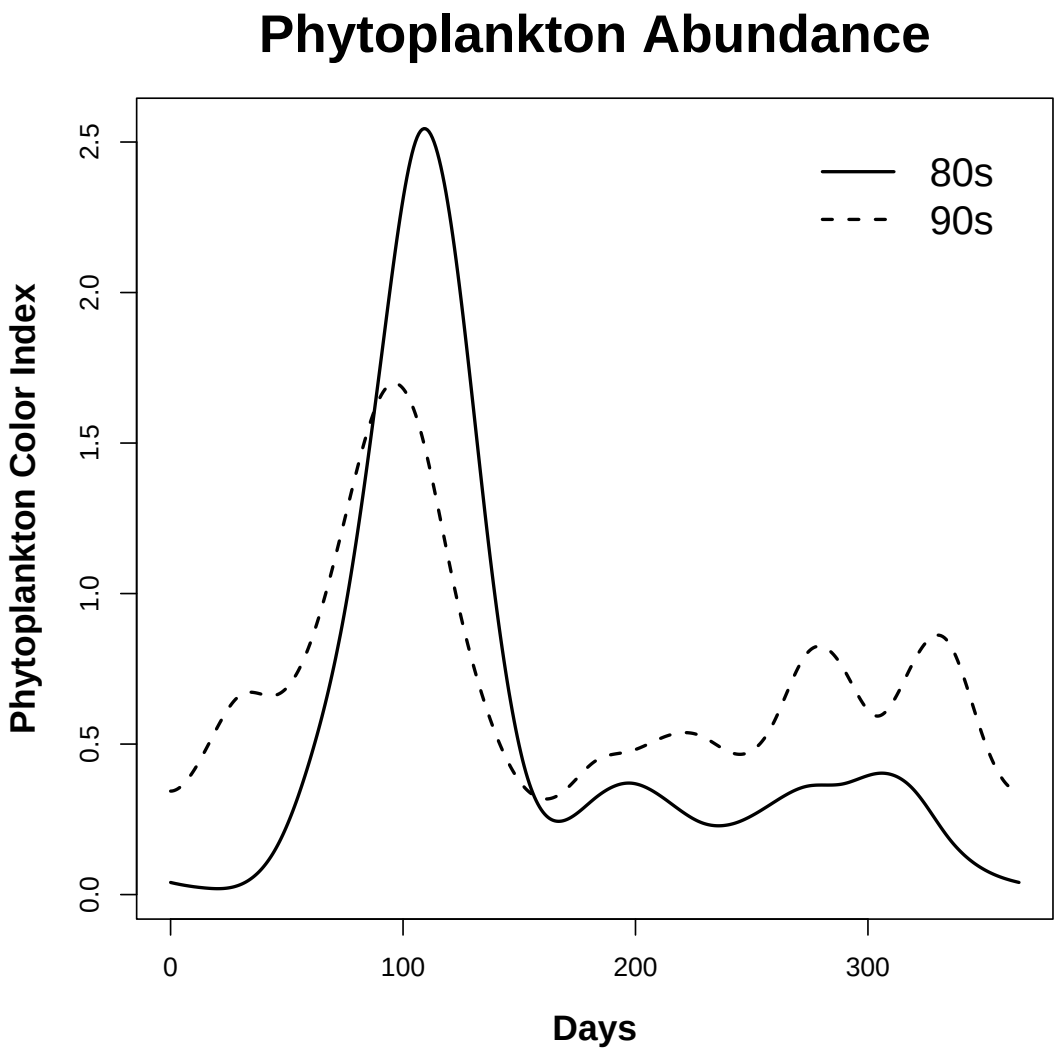


Figure 2.1: Annual patterns of phytoplankton abundance comparing an average year in the 1980s (solid line) to an average year in the 1990s (dashed line). Here, Phytoplankton Color Index (PCI) is used as a proxy for phytoplankton abundance. See 2.4 for more details on PCI and on how data were fit using a model fitting function.

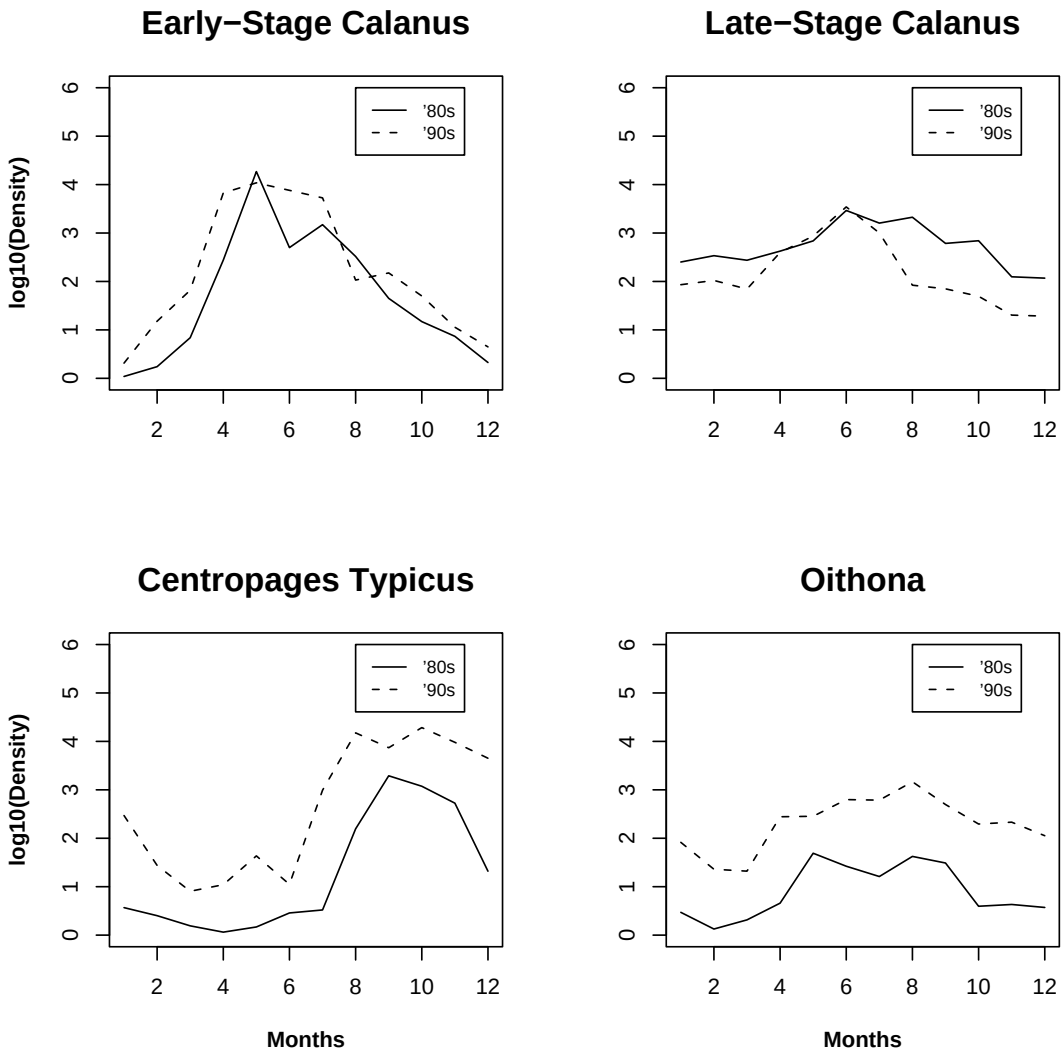


Figure 2.2: Annual patterns of zooplankton abundance comparing an average year in the 1980s versus an average year in the 1990s for *Centropages* (A), *Oithona* (B), early-stage *C. finmarchicus* (C), and late-stage *C.finmarchicus* (D). 1980s abundances are marked by a solid line and 1990s abundances by a dashed line. Early-stage *C. finmarchicus* represents classes C1-C4 copepodites and late-stage represents C5 non-diapause and C6 classes. For each taxon, a periodic spline was fit to the mean monthly values averaged over each decade.

Table 2.1: Two sample t-tests for phytoplankton abundance (PCI), sea surface temperature (SST) and zooplankton comparing the 1980s mean to the 1990s mean. Zooplankton include *Centropages* ,*Oithona* , *C. finmarchicus* stages 1-4 (C1-C4), *C. finmarchicus* stages 5-6 (C5-C6). The *C. finmarchicus* C5-C6 data does not include the diapausing C5 class. A negative $t$ value means that the 1990s had a higher mean than the 1980s for that time period. Two sample t-tests were performed for four different time periods: January-March, April-June, July-September, and October-December. A value of $p > 0.5$ is considered to be non-significant

| | **Jan-Mar** | | | **Apr-Jun** | | | **Jul-Sep** | | | **Oct-Dec** | | |
|---|---|---|---|---|---|---|---|---|---|---|---|---|
| | t | df | p | t | df | p | t | df | p | t | df | p |
| **PCI** | -4 | 543 | << 0.001 | 2.8 | 579 | 0.01 | -2.4 | 589 | 0.02 | -5.6 | 581 | << 0.001 |
| **SST** | 2.48 | 35 | 0.02 | 0.6 | 53 | 0.58 | -0.8 | 54 | 0.42 | -0.17 | 54 | 0.86 |
| **Ctyp** | -4.7 | 545 | << 0.001 | -6.4 | 574 | << 0.001 | -9.6 | 615 | << 0.001 | -9 | 601 | << 0.001 |
| **Oith** | -6.4 | 545 | << 0.001 | -6 | 574 | << 0.001 | -6.1 | 615 | << 0.001 | -9 | 601 | << 0.001 |
| **C1-C4** | -4.6 | 545 | << 0.001 | -2.9 | 574 | 0.006 | -2.6 | 615 | 0.01 | -1.2 | 601 | 0.22 |
| **C5-C6** | 8.1 | 545 | << 0.001 | -2.4 | 574 | 0.02 | 5.8 | 615 | << 0.001 | 8.6 | 601 | << 0.001 |

### 2.3.2 Hypotheses 1: Top-down processes suppress late-stage *C. finmarchicus*

The shift in plankton abundance was reflected in increased abundances higher up the food chain among several species of fish including yellowtail, witch flounder and winter flounder (48). Herring in particular exhibited a remarkable jump in density increasing to ten times the mean abundance of the 1980s (45; 46). This was in part a result of the decrease in fishing effort on herring in the late 1970s, due to the exclusion of foreign fleets. Reduced fishing mortality allowed for a steady recovery of herring over the last three decades. In addition, herring exhibited an increase in larval recruitment into adulthood starting in the late 1980s which also aided in their recovery(53).

Although multiple fish species consume *C. finmarchicus* at some stage in their development, herring are known to feed on *C. finmarchicus* throughout their life-time. Limited by the size of their mouth parts, herring larvae feed on the naupliar stages of small copepods available to them including *Centropages typicus*, *Oithona* spp. and early copepodite stages of *C. finmarchicus* (11). However, once they reach the juvenile and adult stages, mouth parts become larger and more developed and adult herring preferentially feed on late-stage *C. finmarchicus* (14). There are a variety of mechanisms by which herring feed. They are able to use their gill rakers to filter-feed as well as visually detect larger prey and attack through biting (3; 19). Considering the tenfold increase in the standing stock biomass of adult herring in the 1990s, it is conceivable that herring played a key role in reducing late-stage *C. finmarchicus*.

### 2.3.3 Hypotheses 2: Bottom-up processes suppress late-stage *C. finmarchicus*

An alternative hypothesis is that bottom-up process are entirely responsible for the shifts observed in the 1990s. *C. finmarchicus* has 13 developmental stages: egg, 6 nauplii (N1-N6), 5 copepodid (C1-C5) and adult(C6). At the end of the C4 stage, *C. finmarchicus* will develop into one of two types of C5 copepodids: diapause (C5D) and non-diapause (C5ND). C5D will migrate to depths below 150 m (5) where they will remain for up to six months before emerging and becoming adults. C5ND will remain in the top 50 meters (28), molt into adulthood within two weeks and begin reproducing.

In the Gulf of Maine there are two generations of *C. finmarchicus* per year. The first generation begins to emerge in January and reaches the C4 stage 2-3 months later (37). At this point some fraction transition into diapause and migrate to deeper waters where they remain for the next 3-6 months. The rest remain at the surface as C5ND, giving rise to the the second generation (40). The second generation typically reaches the end of the C4 stage in mid-July and again, some fraction go into diapause while the rest become C5ND. By late August most of the population (about 90%) is in diapause (40; 52).

There is much debate as to what proportion of C4s transition into diapause and what processes governs this transition. One possible explanation is that the amount of available phytoplankton acts as a direct cue for diapause entry. (28) for suggest that if food concentrations are below a critical threshold at the end of the C4 developmental stage, *C. finmarchicus* will enter into the C5D class to avoid bad conditions. A second hypothesis is that if a developing *C. finmarchicus* has not

attained enough lipid stores by the time it reaches the end of the C4 development stage, it will not be able to enter diapause. Instead the copepodid will remain at the surface as a C5ND (31). Under this hypothesis, *C. finmarchicus* is more likely to enter diapause when food conditions are good. Speirs ruled out food dependence as a mechanism for transition in favor of the idea that, at any given time, a fixed fraction (70%) enter diapause regardless of available food while the rest enter into C5ND (52).

## 2.4 Model Description

### 2.4.1 Model Overview

Our model is a two dimensional ordinary differential equation, focused on abundances across an average year in the 1980s versus an average year in the 1990s for late-stage C5 non-diapause (C5ND) and adults (C6). The C5 diapause (C5D) class is not included in the model because we do not have data for this class. The model equations are:

$$\begin{aligned} \frac{dC_5}{dt} &= p\frac{C_4(t)}{D_4(T)} - GH(t)\frac{C_5}{q + C_5 + C_6} - \left(\frac{1}{D_5(T)} + m_5(T)\right) C_5 \\ \frac{dC_6}{dt} &= \frac{C_5}{D_5(T)} - GH(t)\frac{C_6}{q + C_5 + C_6} - m_6(T)C_6. \end{aligned} \tag{2.1}$$

This set of equations represent the rate of change of C5ND and C6 densities over time, so that:

$\frac{dC_5}{dt}$ = maturation from C4 to C5ND - predation - maturation to C6 - mortality

$\frac{dC_6}{dt}$ = maturation from C5ND to C6 - predation - mortality.

C4 abundance, $C_4(t)$, and adult herring abundance, $H(t)$ are not explicitly modeled but instead are exogenous variables represented by a time series of data which gets fed directly into the model. At any given time period, some fraction of the C4 class, $p$, transition into the C5ND. The formulation for $p$ depends on which definition of transition is being modelled (either food-dependent of food-independent). Both the development rates through the end of a stage, $D_i(T)$, and mortality rate, $m_i(T)$ are functions of sea surface temperature (SST), $T$. In the predation term the consumption rate of adult herring is expressed by $G$, and $q$ represents the half-saturation constant (a measure of how efficiently predators consume their prey). We continue our discussion of how vital rates are defined below. (For more details on specific parameter values see Tables 2.2 and 2.3).

Table 2.2: *Calanus* parameter values determined either through model fits or from the literature. All parameters are dimensionless constants unless specified.

| Parameter | Description | Value | Source |
|---|---|---|---|
| *Development Parameters* | | | |
| $\beta$ | Exponent for Belehrádek function | -2.05 | Campbell et al. (2001) |
| $T_d$ | temperature standard for Belehrádek function | 9.11 | Campbell et al. (2001) |
| $a_4$ | Belehrádek constant | 8798 | Campbell et al. (2001) |
| $a_5$ | Belehrádek constant | 10964 | Campbell et al. (2001) |
| $a_6$ | Belehrádek constant | 15047 | Campbell et al. (2001) |
| *Mortality Parameters* | | | |
| $d_5$ | C5 baseline mortality value | $0.15d^{-1}$ | Eiane (2002) |
| $d_6$ | C6 baseline mortality value | $0.01d^{-1}$ | Eiane (2002) |
| $T_c$ | critical temperature for mortality | — | Optimized (see Table 2.4) |
| $C_l$ | low phytoplankton-related transition threshold | — | Optimized (see Table 2.4) |
| $C_h$ | high phytoplankton-related transition threshold | — | Optimized (see Table 2.4) |
| z | exponent for temperature-dependent mortality | 7 | Speirs et al. (2006) |
| $\gamma_0$ | fraction background mortality at 0° Celsius | 0.65 | Speirs et al. (2006) |

Table 2.3: Herring parameter values determined either through model fits or from the literature.

| Parameter | Description | Value | Source |
|---|---|---|---|
| q | predator half-saturation constant | | optimized (see Table 2.4) |
| $Hkg_{80}$ | ave. biomass of age 2+ in the 1980s (mt) | $1.9 \times 10^8$ | Overholtz (2001) |
| $Hkg_{90}$ | ave. biomass of age 2+ in the 1990s (mt) | $7.5 \times 10^8$ | Overholtz (2001) |
| $Hwt_{80}$ | ave. weight of age 2+ in the 1980s (kg) | 0.24 | Overholtz et al. (2004) |
| $Hwt_{90}$ | ave. weight in the 1990s (kg) | 0.18 | Overholtz et al. (2004) |
| $sa$ | surface area of the Gulf of Maine ($m^2$) | $5.9 \times 10^{10}$ | NEFSC |
| $Cmax$ | max. consumption (g zoop./g fish/day) | 0.13 | McCann (1998) |
| $f$ | fraction of Cmax at which fish consumes | 0.7 | McCann (1998) |
| $wt_5$ | C5 dry weight (g) | $1.7 \times 10^{-4}$ | Speirs et al. (2006) |
| $wt_6$ | C6 dry weight (g) | $2.8 \times 10^{-4}$ | Carlotti et al. (1993) |
| $G$ | number zoop. eaten $day^{-1}$ | $(Awt \times Cmax \times f)/wt_i$ | McCann (1998) |

### 2.4.2 Model Assumptions

As described in section 2.3.3, the mechanism for development from C4 to C5ND is defined in one of three ways: (1) C4 class developes into the C5ND class and remain at surface when food abundance is low because they do not have enough lipid stores to enter into diapause (31); (2) C4 class developes into C5ND and remain at surface when there is enough available food for reproduction and otherwise, enter diapause when conditions are bad (28); (3) C4 class developes into C5ND at a fixed fraction,$p = 0.3$ (52). Throughout the remainder of this paper, we refer to the three model descriptions of transition from C4 to surface C5ND in the following way: (1) "Low Food Surface" (31), (2) "High Food Surface", and (3) "Fixed Surface". Each model is split into three cases to explore the relative roles of top-down and bottom up controls on *C. finmarchicus*: (a) both phytoplankton availability and density of adult herring was different between decades("All Different"); (b) herring abundance was different in the 1990s, but phytoplankton abundance remained the same across both decades ("Food Same"); (c) phytoplankton abundance was different, but herring abundance remained the same across both decades("Fish Same"). We look at a $3 \times 3$ comparison examining each of the three model descriptions across the three cases which describe the relative impact of top-down verses bottom up processes. For clarity, throughout the duration of this paper we define each of the nine combinations of "model, case" as a scenario. For the last two cases ("Food Same" and "Fish Same"), "Same" is defined as the climatological herring and phytoplankton abundance (long-term average conditions across both decades). "Differ" means that a separate average is determined for each decade.

Estimated values for the initial densities of C5ND and C6 were obtained from the literature (37). It is assumed that the C5ND class is the emerged over-wintering

diapause class from the previous year which molts into the adult class and begins to reproduce. January 1st is equivalent to day 1 in the model, which is a reasonable assumption, given that, in the Gulf of Maine, *C. finmarchicus* can begin emergence from diapause as early as the end of December (31). Different initial conditions are given to the 1980s model versus the 1990s model to account for the fact that the initial populations of emerging C5 in January were smaller in the 1990s than in the previous decade. Initial values were determined by using monthly averages in January for both decades as a rough estimate.

### CPR Time Series Data

Information about seasonal *C. finmarchicus* and phytoplankton abundances comes from the Continuous Plankton Recorder (CPR) survey conducted by the National Marine Fisheries Service from 1961-present (32). The CPR instrument is towed behind commercial ships and samples the top $\approx 10$ m of the water column. As a result, the data set does not include information on the C5 diapause class which are located at about 150 m. The survey is conducted one to two times a month along a 500 km transect from Boston, Massachusetts to Yarmouth, Nova Scotia. The data for each species includes information on: zooplankton abundance (individuals $m^{-3}$), date, latitude, longitude, distance from Boston along trackline (km), time of day, and PCI (Phytoplankton Color Index) which ranks phytoplankton abundance on a scale from 1 to 3. A PCI of 3 represents approximately 6.5 times the concentration of PCI=1 (2). According to statisistical analysis (see Table 2.1), PCI is significantly higher in the 1990s between July-March and higher in the 1980s between April-June.

Copepods captured by the CPR are often damaged, making it difficult to obtain

abundance data for individual developmental stages, particularly for the smaller species and early developmental stages. The CPR data therefore do not fully distinguish the individual stages of *C. finmarchicus*. Instead, copepodid stages 1-4 are grouped, as are stages 5-6. Also the C1-C4 do not specify particular *Calanus* species. However, other species in the *Calanus* genus (e.g. *C. glacialis*) are rare in the Gulf of Maine; we therefore assume that the bulk of the C1-C4 class are comprised of *C. finmarchicus*. When we refer to *Calanus* throughout the duration of this paper then, we are referring particularly to the *C. finmarchicus* species.

The model requires a time series for C4 abundance, isolated from the C1-C4 data provided by the CPR survey. To estimate the proportion of C4s in the CPR sample, we need to know what fraction of the C1-C4 class are C4s and how this changes as a function of time. To accomplish this we utilize a fully stage-resolved data set of *C. finmarchicus* from 2003-2007 collected at multiple stations in the Gulf of Maine (Jeff Runge & Rebecca Jones, unpublished data). From this data set, we obtain the fraction of C4s at each station on every date that data was collected. A local polynomial regression is then used to fit the data and obtain a relationship for how the fraction of C4 abundance changes over time relative to the C1-C4 total, $f_{C_4}(t)$. The next step is to generate a function describing the change in abundance of the C1-C4 class over time, $C_{1-4}(t)$, for a typical year in the 1980s and the 1990s. We do this by finding a monthly average across the entire trackline for each data and then using linear interpolation between these points to obtain a function of C1-C4 abundance over time. An expression for how C4 abundance changes throughout time can be found by letting

$$C4(t) = f_{C_4}(t) \times C_{1-4}(t). \tag{2.2}$$

Figure 2.3 shows how the fraction of C4 abundance changes with respect to time relative to total C1-C4 abundance (a), as well as the difference in C4 abundance

between the 1980s and the 1990s, where abundances are measured in individuals $m^{-3}$.

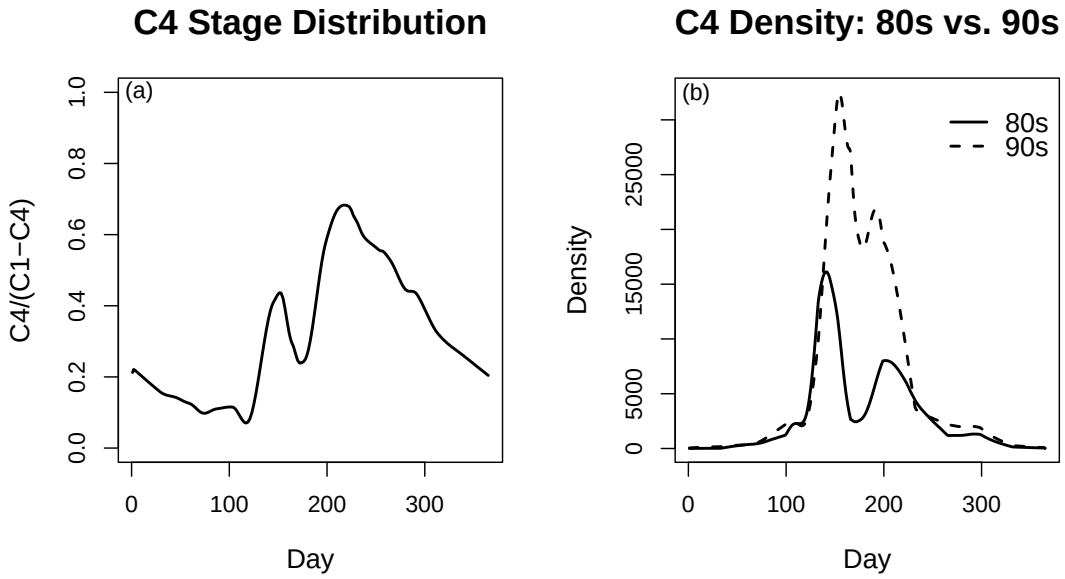


Figure 2.3: (a) Fraction of the C1-C4 class that are C4 (from J. Runge and R. Jones). (b) Time series of C4 density (individuals $m^{-3}$) for 1980s verses 1990s.

For the "Low Food Surface" and "High Food Surface" models, where transition probability is a function of food, we need some quantifiable measure of phytoplankton. Chlorophyll-a values, a standard proxy for phytoplankton abundance, are not available for both decades. However, the PCI from CPR survey is available for the entire period. Although PCI is not ideal, it does provide a consistent estimate of phytoplankton abundance, one that is correlated with fluorometric measurements of chlorophyll-a (2). In addition, the annual patterns displayed by the PCI are consistent with known patterns of phytoplankton abundance in the GOM between decades. To find an average phytoplankton abundance for each decade, the year portion of the data is removed so that each observation is given as some percent-

age of the year across all regions. The data are then fitted using a model fitting function (generalized additive model), which yields a relationship between phytoplankton abundance and time. Using this relationship, a series of abundance values were generated at multiple time steps for a typical year in the 1980s and a typical year in the 1990s. (For the "Food Same" case, we obtained the climatological abundance across both decades.) Given this set of predicted values of seasonal phytoplankton abundance, linear interpolation is employed to derive a function for the dependence of PCI on time.

### Sea Surface Temperature

To obtain daily estimates of mortality and development rates, temperature observations were extracted from the Bedford Institute of Oceanography's Climate Database (26). Similar to the calculations for phytoplankton and C4 abundance, a model fitting function was used to determine the relationship between temperature and time. From this a time series of expected observations describing an average year in the 1980s and the 1990s was obtained. Linear interpolation was used to create an expression for temperature as a function of time from these predicted values. Figure 2.4 shows the annual mean temperature across the 1980s and 1990s and highlights the decrease in winter temperature in the 1990s that were associated with increased Scotian Shelf water during this time period. Only SST from January-March exhibit a significant difference between decades, with temperatures colder in the 1990s during this period (see Table 2.1).

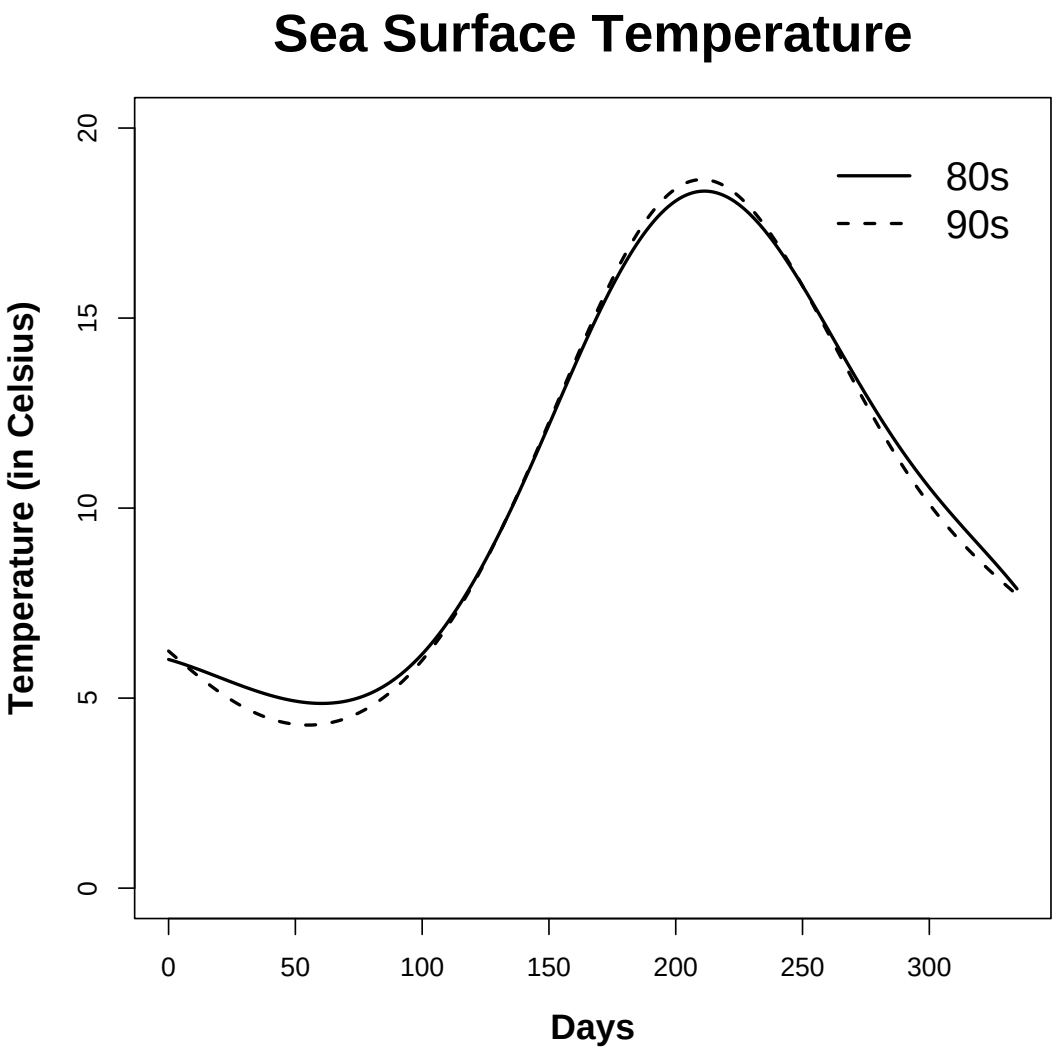


Figure 2.4: Annual patterns of Sea Surface Temperature using in situ data. For each decade, a periodic spline was fit to the entire data set.

**Mortality**

Although relatively little is known about the mortality rates of *Calanus finmarchicus* and the processes governing these rates (44; 52), there is some evidence of a positive relationship between temperature and mortality (30; 42). To reflect this relationship, background mortality rate, $m_i$, for each stage $i$, is described as an

Table 2.4: The optimized values for the three cases ("All Differ", "Food Same", "Fish Same") of each model ("Low Food Surface", "High Food Surface", "Fixed Surface").

| | Critical temperature $T_c$ | Herring half-saturation $q$ | Low food threshold $C_l$ | High food threshold $C_h$ |
|---|---|---|---|---|
| *"Low Food Surface" Model* | | | | |
| All Differ | 10.17° C | 1736 | 0.314 | 0.317 |
| Food Same | 11.47° C | 1008 | 0.041 | 0.150 |
| Fish Same | 9.98° C | 1845 | 0.281 | 0.380 |
| *"High Food Surface" Model* | | | | |
| All Differ | 11.25° C | 1685 | 3.054 | 3.071 |
| Food Same | 11.2° C | 1651 | 3.918 | 3.945 |
| Fish Same | 11.06° C | 2385 | 3.510 | 3.538 |
| *"Fixed Surface" Model* | | | | |
| All Differ | 9.84° C | 653 | — | — |
| Food Same | 9.79° C | 646 | — | — |
| Fish Same | 9.75° C | 983 | — | — |

increasing function of temperature.

$$m_i = \gamma(T) d_i \tag{2.3}$$

and

$$\gamma(T) = \gamma_0 + (1 - \gamma_0) \left( \frac{T}{T_c} \right). \tag{2.4}$$

This is a simplified, density-independent and food-independent version of a function described by (52). Density-dependent mortality is not included as the model focus on the later classes and density-dependence is believed to be important only in the early stages of *Calanus* (44).

The parameter $d_i$ represents the specific nominal mortality rate for stage $i$ (16). $T$ is sea surface temperature in Celsius. We use the mortality at $T_c$ as a baseline, where, when $T = T_c$, $\gamma(T) = 1$. Given this, $\gamma_0$ represents the fraction of mortality rate experienced by *C. finmarchicus* at 0° Celsius relative to the mortatiliy rate at $T_c$. The values for $d_i$ and $\gamma_0$ come directly from the literature and are specified in Table 2.2. The value for $T_c$ is estimated by maximum likelihood (see Section 2.4.3 and Table 2.4 for more details).

**Development Time**

The development time from one class into the next, which is a function of SST, is defined using a slighlty modified version of the Belehrádek equation:

$$Dev_i = a_i (T + T_d)^{\beta}. \tag{2.5}$$

In the original equation, $Dev_i$ is the time from the midpoint of the egg-laying period to the time when 50% of the copepods have reached a given stage. The parameter, $a_i$, is an empirically derived stage-specific constant taken from (9). For

our purposes, we want to look at the the length of time it takes to develop through each stage. As such, we define development, $D_i$ as

$$D_i = a_{i+1}(T + T_d)^{\beta} - a_i(T + T_d)^{\beta}, \tag{2.6}$$

where $i$ represents the stage of interest. Specific values for $a_i$, $T_d$ and $\beta$ can be found in Table 2.2.

**Fraction that transition from C4 into C5 non-diapause**

Development from the C4 to the C5ND class is defined in three different ways: (1)"Low Food Surface": here, the fraction entering into the surface C5ND class is represented by a decreasing function of food availabilty. Under these assumptions, C4s cannot tansition into diapause when food is low because they do not have sufficient lipid stores to do so. Instead they enter the C5ND class and remain at the surface. The fraction remaining at the surface as a C5ND, $p$, is defined as follows:

$$p = \begin{cases} p_h & \text{if } c(t) \leq C_l \\ \frac{p_h - p_l}{C_l - C_h}(c(t) - C_l) + p_h & \text{if } C_l < c(t) < C_h \\ p_l & \text{if } c(t) \geq C_h \end{cases} \tag{2.7}$$

Equation 2.7 states that if phytoplankton abundance is below a minimum food threshold ,$c(t) < C_l$ (where $c(t)$ represents phytoplankton abundance), then most of the C4s ($p_h = 0.9$), will mature into C5ND. As the amount of available food increases, the fraction of C4s that develop into C5ND gradually decreases. For $c(t) > C_h$ the fraction of C4s that develop into the C5ND drops to $p_l = 0.1$. We have set the particular values for $p_h$ and $p_l$ to reflect the fact that by late August-early September, most *Calanus* (approximately 90% according to (40)) have entered into diapause . The parameters, $C_l$ and $C_h$, represent critical low

and high Phytoplankton Color Index which determine the fraction of C4s that transition into C5ND. Specific values for $C_l$ and $C_h$ are found through maximum likelihood and will thus vary for each model (see Table 2.4).

(2) The fraction of C4s that develop into C5ND, $p$, is an increasing function of available food (i.e. transition into diapause occurs to avoid bad conditions). When food is abundant, C4s enter into surface C5ND, molt within two weeks into adults and start reproducing. The fraction, $p$, is now defined as:

$$p = \begin{cases} p_l & \text{if } c(t) \leq C_l \\ \frac{p_h - p_l}{C_h - C_l}(c(t) - C_l) + p_l & \text{if } C_l < c(t) < C_h \\ p_h & \text{if } c(t) \geq C_h \end{cases} \tag{2.8}$$

where again, $p_h = 0.9$, $p_l = 0.1$. In this case, the fraction of C4s that develop into C5ND is small when phytoplankton abundance is low but increases linearly with increasing phytoplankton abundance.

(3) The fraction of the C4 class entering into C5ND is fixed at $p = 0.3$ independent of available food. The fraction which stay at the surface, $p$ comes from (52) and is derived through model fits.

**Herring Abundance**

In order to obtain the correct units for our model, the biomass data available must be converted to represent the number of individual herring $m^{-3}$. Biomass information was obtained from a NMFS herring stock assessment (45) which represents abundance in metric tons (mt). Using an average value for each decade, we estimate an abundance of 190,000 mt (metric tons) for the 1980s and 750,000 mt for the 1990s. The total biomass for each decade is converted to kg (1 mt = 1000

kg) and then divided by the average weight in kg of an adult fish. Data from the Northeast Fisheries Science Center (46) was used to determine the average weight for an adult fish in the 1980s versus the 1990s, which gives the average weight for each age class per year. This data set ranges back to 1967, allowing for a separate calculation of mean adult weight for each decade. Average adult weight was calculated using only data for ages 2+ (see Table 2.3). Given the total number of fish in the region for each decade, total abundance is then divided by the total surface area of the GOM in meters squared to get adult herring $m^{-2}$ ($3.2 \times 10^{-5}$ in the 1980s and $7 \times 10^{-2}$ in the 1990s).

Annual variation in herring abundance is described using seasonal distribution data derived from NOAA's Estuarine Living Marine Resources (ELMR) progam as a rough guide for when herring are present in the region. The ELMR data set spans the years between 1985-2000 and gives information on average patterns of seasonal abundance and distribution of various species of fishes and vertebrates. This data set includes bays and estuaries in each region (West Coast, Gulf of Mexico, Southeast, Mid-Atlantic, and North Atlantic) of the continental U.S., based on their ecological and economic importance. For each location, a monthly abundance for each species is determined, where abundance is relative to the same life stage of other similar species within a pre-determined guild (see (43) for more information on how this data set was obtained). From this data set, Penobscot Bay in the NW Gulf of Maine is chosen as a representative region. The relative abundance of herring is defined on a scale from 0 to 5 (0=Absent, 5=Highly Abundant). According to this data set, herring are present in Penobscot Bay monthly as follows:

| Jan | Feb | Mar | Apr | May | Jun | Jul | Aug | Sept | Oct | Nov | Dec |
|---|---|---|---|---|---|---|---|---|---|---|---|
| 3 | 3 | 3 | 4 | 5 | 5 | 5 | 5 | 5 | 5 | 4 | 3 |

Letting a score of 5 represent twice the abundancance of the average value of herring $m^{-2}$ derived from the NMFS data gives a range of ($3.2 \times 10^{-5} m^{-2}$, $6.8 \times 10^{-5} m^{-2}$) for the 1980s herring abundance and ($7 \times 10^{-2} m^{-2}$, $1.4 \times 10^{-1} m^{-2}$) for the 1990s. The final step is to convert these estimates to number of individuals $m^{-3}$. This is done by dividing the number of herring $m^{-2}$ by 50 m, the assumed depth of surface zooplankton (28).

In equation (2.1), herring consumption rate, $G$ is defined as (grams of zooplankton eaten) (gram of fish)$^{-1}$ (day)$^{-1}$. This number is then converted into (ind. zooplankton eaten) (fish)$^{-1}$ (day)$^{-1}$. The above formulation for consumption rate was obtained from a modeling paper by McCann (36) which describes the feeding rate for all opportunistic fishes, including herring (see Table 2.3 for more details). The half-saturation constant, $q$, in the functional response equation has been fitted for each model (see Table 2.4).

### 2.4.3 Optimizing parameters and quantifying model fits

Our model contains several free parameters which are not known from the literature and not fixed at any particular value by the model hypotheses. These include the critical temperature, $T_c$ which appears in the mortality equation; the adult herring half-saturation constant, $q$ in the functional response equation; and for the food dependent models, $C_l$ and $C_h$, which determine the conditions for developing from the C4 to the C5ND class. These four parameters are also logical choices for optimization because they directly relate to our two hypothesis about the importance of predation versus climate driven changes in the system.

Optimal parameter values are found by minimizing the residuals between the

model and data for the 1980s verses the 1990s. To find the residuals, simulations are run for a representive year for each decade, from which log-transformed weekly averages of total late stage *C. finmarchicus* density were obtained. In order to find the log-likelihood estimate, it is necessary to know whether the residuals are normally distributed or not. This can be determined by running a Wilks-Shapiro normality test. Tunning this test showed that the residuals were normally distributed with a mean equal to 0 and a standard deviation of 0.42.

Once a log-likelihood estimate is found for each model, these estimates are used to find the model which minimizes the Akaike Information Criterion (AIC), defined as

$$AIC = -2L + 2k, \tag{2.9}$$

where $L$ is the minimized negative log-likelihood and k represents the total number of parameters optimized in the model (1) In 2.9, $-2L$ reflects the goodness-of-fit of the model to the data and $2k$ is the penalty on the model based on how complex it is (i.e. how many parameters it has).

The advantage of using AIC is that it allows for comparison between models with varying numbers of fitted parameters, $k$. For the cases where $p$ is a food-dependent function ("Low" and "High Food Surface" models), $k = 4$ (fitted parameters: $T_c$, $q$, $C_l$, $C_h$). For the "Fixed Surface" model, there is no definition for $C_l$ and $C_h$, so $k = 2$. The standard formulation for AIC requires that the sample size, $n$, be large relative to the number of fitted parameters in each model, $k$. Because we are comparing weekly abundance averages, this gives a sample size of $n = 52$. According to (8) and (6), if $n/k < 40$, it is then necessary to include an extra penalty on our fits by using a corrected AIC, where

$$AIC_c = AIC + \frac{2k(k+1)}{n-k-1}. \tag{2.10}$$

The model with the lowest $AIC_c$ value will be considered the best fit to the data. AIC measures the loss of information of each candidate model to the best-fitting model

The best fit model can be evaluated relative to all other candidate models by calculating the AIC weights. AIC weights range between 0 and 1, where a weight of 0 represents complete loss of information and a weight of 1 represents no loss of information (27). For each model, $i$, its AIC weight is determined as:

$$w_i = \frac{e^{-.5\times\Delta AIC_i}}{\sum_{j=1}^{m} e^{-.5\times\Delta AIC_j}}, \tag{2.11}$$

where $i$ is the model being evaluate and $m$ are the total number of other models being evaluated. Generally, only the model with the largest AIC weight and the candidate models with weights $> 10\%$ of the largest AIC weight are interpreted (8)

In addition to the AIC values for each model, we can also calculate the Bayesian Information Criterion (BIC):

$$BIC = -2L + k\log(n), \tag{2.12}$$

BIC is a slightly stricter set of criterion in the sense that the penalty for a more complex model is increased when $\log(n) > 2$. We include BIC and $\Delta$BIC values in our analysis of goodness-of-fit of each scenario.

## 2.5 Results

### 2.5.1 AIC: Comparing model fits

The best fit to the data across all models is the "Low Food Surface, All Differ" scenario, with a $\Delta$AIC value of 20.76 between this scenario and the second best fit scenario, "Low Food Surface, Fish Same" (Table 2.5). The fact that the AIC weight for "Low Food Surface, All Differ" is very close to 1 (0.999) reflects our confidence in this model being the most accurate description of the data. The second thing to note about the outcomes of the AIC comparisons is that the models which incorporate development into C5ND as a function of available food (i.e., "Low Food Surface" and "High Food Surface" models) are almost uniformly better fits to the data than the model which assumes no food dependence (i.e., "Fixed Surface") . This pattern holds true for comparisons across all three cases of the "Low Food Surface" model (i.e. "All Differ", "Food Same", "Fish Same") and two of the three cases of the "High Food Surface" model (i.e. "All Differ", "Food Same"). For all three cases of the "Fixed Food Surface" model, $\Delta$AIC is very large. In fact the lowest AIC value among these three cases, "Fixed Surface, All Differ", has a $\Delta$AIC=47.34 when compared to the "Low Food Surface, All Differ" scenario. All of these major results hold for the BIC comparisons as well, with the "Low Food Surface, All differ" again being clearly the best fit to the data.

For within model comparisons of AIC values across all three cases of each model (i.e. "All Differ", "Food Same, "Fish Same"), the "All Differ" case is the best fit to the data for each of the three models. This is particularly true for the "Low Food Surface model, where the $\Delta$AIC value between the best fit and 2nd best fit models is 20.76. For the "High Food Surface" and "Fixed Surface" Models these

Table 2.5: Comparison of all models to the data - BIC vs. AIC. The first column gives the negative log-likelihood of the residuals (L), column 2 shows the number of fitted parameters in each scenario, column 3 shows the BIC values and the $\Delta$BIC values giving the difference between the best-fit models and other candidate models is in column 4, column 5 shows the AIC values (using the corrected AIC for small sample size), column 6 gives the $\Delta$AIC values, column 7 gives the AIC weights.

| | L | # Parameters fitted | BIC | $\Delta$BIC | $AIC_c$ | $\Delta AIC_c$ | AIC weight |
|---|---|---|---|---|---|---|---|
| Low Food Surface, All Differ | 76.44 | 4 | 168.69 | 0.00 | 161.73 | 0.00 | 0.999 |
| Low Food Surface, Fish Same | 86.88 | 4 | 189.57 | 20.88 | 182.61 | 20.76 | $3 \times 10^{-5}$ |
| High Food Surface, All Differ | 89.05 | 4 | 193.91 | 25.22 | 186.94 | 25.21 | $3 \times 10^{-6}$ |
| Low Food Surface, Food Same | 90.26 | 4 | 196.33 | 27.64 | 189.36 | 27.63 | $1 \times 10^{-6}$ |
| High Food Surface, Food Same | 91.06 | 4 | 197.93 | 29.24 | 190.97 | 29.24 | $4 \times 10^{-7}$ |
| Fixed Surface, All Differ | 102.41 | 2 | 212.72 | 44.03 | 209.07 | 47.34 | $5 \times 10^{-11}$ |
| Fixed Surface, Food Same | 103.97 | 2 | 215.84 | 47.15 | 212.18 | 50.45 | $1 \times 10^{-11}$ |
| High Food Surface, Fish Same | 111.50 | 4 | 238.81 | 70.12 | 231.85 | 70.12 | $6 \times 10^{-16}$ |
| Fixed Surface, Fish Same | 127.69 | 2 | 263.28 | 94.59 | 259.62 | 97.89 | $6 \times 10^{-22}$ |

differences are much smaller, but still significant ($\Delta$AIC=3.03 and $\Delta$AIC=3.11, respectively). For the "High Food Surface" and "Fixed Surface" models, the cases which include differences in herring abundance ("All Differ" and "Food Same") between the 1980s and 1990s do a better job of matching the data then the case which does not ("Fish Same"). In the "Low Food Surface" model, the "Fish Same" case is actually significantly better than the "Food Same" case.

Table 2.6: Within model comparison across the three cases of each model, comparing each scenario to the data. The first column gives the negative log-likelihood of the residuals (L), BIC values are given in column 2, $\Delta$BIC value are in column 3, column 4 shows the corrected AIC values and column 5 gives the $\Delta$AIC.

| | L | BIC | $\Delta$BIC | $AIC_c$ | $\Delta AIC_c$ |
|---|---|---|---|---|---|
| *Low Food Surface:* | | | | | |
| All Differ | 76.44 | 168.69 | 0.00 | 161.73 | 0.00 |
| Fish Same | 86.88 | 189.57 | 20.88 | 182.61 | 20.76 |
| Food Same | 90.26 | 196.33 | 27.64 | 189.36 | 27.63 |
| *High Food Surface:* | | | | | |
| All Differ | 89.05 | 193.91 | 0.00 | 186.94 | 0.00 |
| Food Same | 90.26 | 197.93 | 4.02 | 190.97 | 3.03 |
| Fish Same | 111.50 | 238.81 | 18.81 | 231.85 | 44.91 |
| *Fixed Surface:* | | | | | |
| All Differ | 102.41 | 212.72 | 0.00 | 209.07 | 0.00 |
| Food Same | 102.64 | 215.84 | 22.97 | 212.18 | 3.11 |
| Fish Same | 127.69 | 263.28 | 47.44 | 259.62 | 50.55 |

According to the data, surface populations of late stage *C. finmarchicus* were lower in the 1990s than in the 1980s for most of the year except in the spring when the abundances were about the same between decades 2.2. This pattern of abundance is fairly accurately captured by all three models ("Low Food Surface", "High Food Surface", and "Fixed Surface") for cases that include changes in phytoplankton and herring ("All Differ") and changes in herring alone ("Food Same") (Figures 2.5, 2.6 and 2.7). For the "Fish Same" case, only the "Low Food Surface"

model matches the changes in seasonal patterns of abundance between the 1980s and the 1990s across the entire year. In this regard, both the "High Food Surface, Fish Same" and "Fixed Surface, Fish Same" scenarios are clearly the worst fits to the data. This is apparent not only by within model comparisons of $\Delta$AIC (44.91, and 50.55 respectively) but also by viewing the model results for the "Fish Same" case in Figures 2.6 and 2.7. For the "High Food Surface, Fish Same" scenario, the 1990s *Calanus* abundances are similar to the data (i.e. lower than the 1980s) for the first three months of the year, but higher than the 1980s for the duration of the year. For the "Fixed Surface, Fish Same" scenario the 1990s late stage *Calanus* abundance is only below the 1980s for approximately the first 30 days and then is above the 1980s for the rest of the year.

### 2.5.2 Mortality Rates

The background mortality rate of C5ND and C6 *C. finmarchicus* is defined both as a function of daily SST and as a function of the critical temperature, $T_c$ (equation 2.4). Because $T_c$ was chosen as one of the fitted parameters, the mortality rates differ between scenarios. In Table 2.7, the mean daily mortality rates of C5ND and C6 *Calanus* were calculated for all nine scenarios examined, as well as the maximum mortality rate day$^{-1}$, averaged across both decades. The maximum mortality rate corresponds with the peak annual temperature. This maximum is included in the table to highlight the range of mortality rates for each scenario.

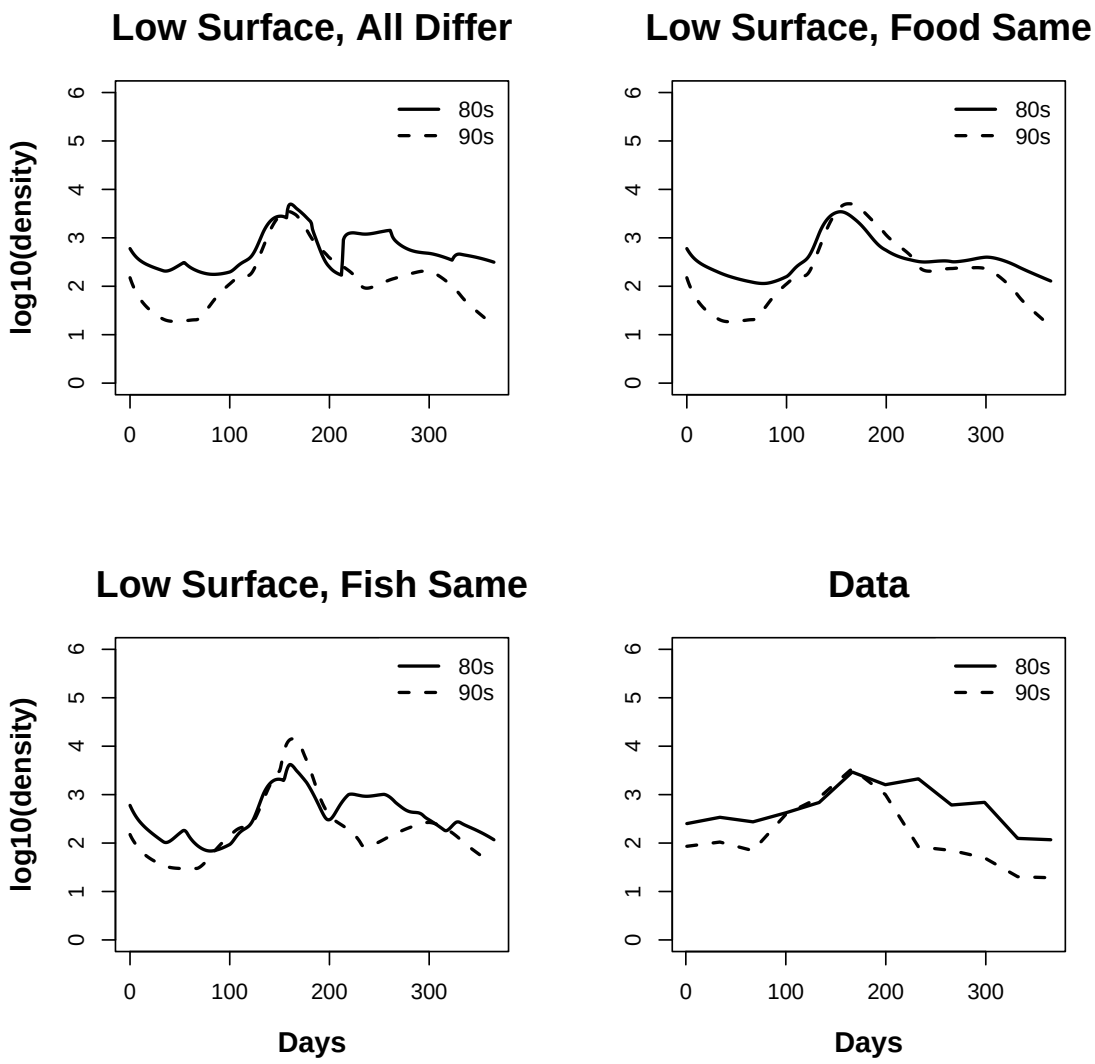


Figure 2.5: Model vs. data comparisons for the "Low Food Surface" model which describes transition from C4 to C5ND as a decreasing function of food. Each panel shows the late-stage *C. finmarchicus* abundance in the 1980s (solid line) vs. 1990s (dashed line). The model was tested under three cases: (1) "All Differ" - Both phytoplankton and herring abundance increased in the 1990s (**A**); (2) "Food Same" - herring abundance increased in the 1990s, but phytoplankton did not not (**B**); (3) "Fish Same" - phytoplankton abundance increased in the 1990s, but herring did not (**C**). Panel **D** shows the average total late stage abundance for each decade from the data.

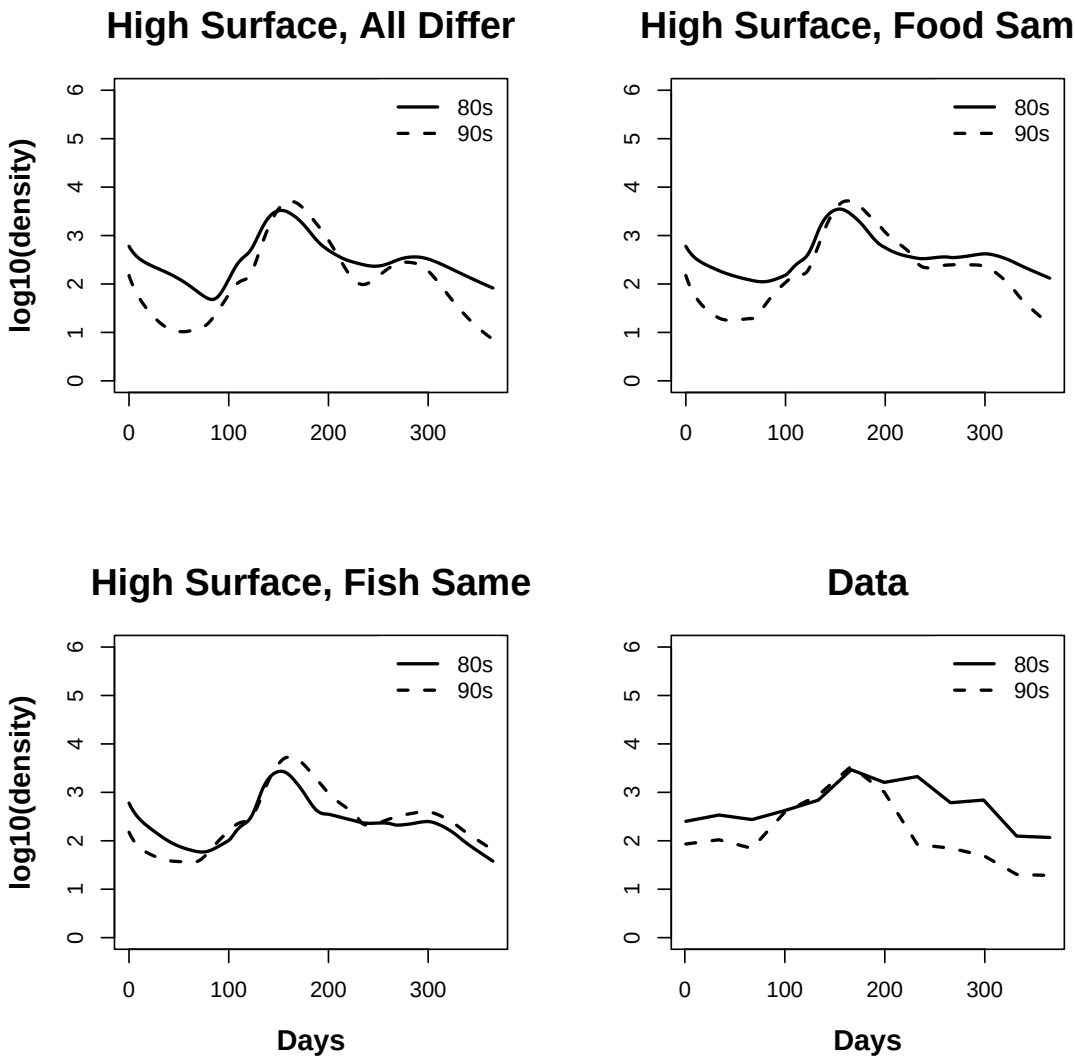


Figure 2.6: Model vs. data comparisons for the "High Food Surface" model which describes transition from C4 to C5ND as an increasing function of food. Each panel shows the late-stage *C. finmarchicus* abundance in the 1980s (solid line) vs. 1990s (dashed line). The model was tested under three cases: (1) "All Differ" (**A**); (2) "Food Same" (**B**); (3) "Fish Same" (**C**). Panel **D** shows the average total late stage abundance for each decade from the data.

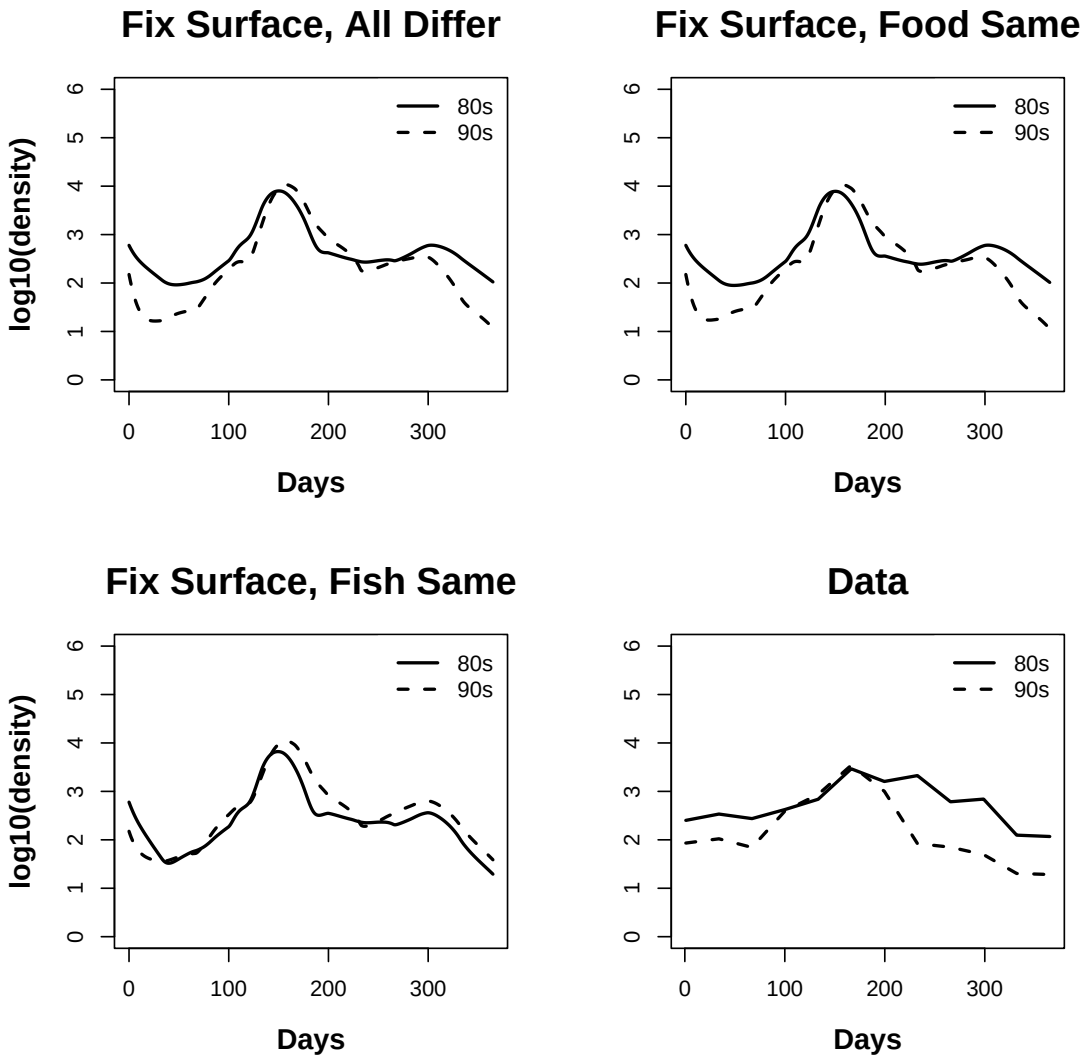


Figure 2.7: Model vs. data comparisons for the "Fix Surface" model which describes transition from C4 to C5ND as food-independent, with a fixed fraction, $p = 0.3$ transitioning into the C5ND class at any given time period. Each panel shows the late-stage *C. finmarchicus* abundance in the 1980s (solid line) vs. 1990s (dashed line). The model was tested under three cases: (1) "All Differ" (**A**); (2) "Food Same" (**B**); (3) "Fish Same" (**C**). Panel **D** shows the data.

Table 2.7: Mortality Rates for the C5ND and C6 classes across all three models. For each case of the model, we calculate the mean mortality rate $d^{-1}$ for the 1980s and 1990s as well as the maximum annual rate for each decade. The maximum rate is given to demonstrate the annual range of mortality rates for each case of the model.

| | **All Differ** | | | **Food Same** | | | **Fish Same** | | |
|---|---|---|---|---|---|---|---|---|---|
| | 80s | 90s | max | 80s | 90s | max | 80s | 90s | max |
| **Low Food Surface Models** | | | | | | | | | |
| C5ND | 0.69 | 0.74 | 3.55 | 0.42 | 0.42 | 1.89 | 0.79 | 0.83 | 4.04 |
| C6 | 0.05 | 0.05 | 0.24 | 0.03 | 0.03 | 0.13 | 0.05 | 0.06 | 0.27 |
| **High Food Surface Models** | | | | | | | | | |
| C5ND | 0.39 | 0.4 | 1.80 | 0.38 | 0.38 | 1.71 | 0.43 | 0.46 | 2.02 |
| C6 | 0.03 | 0.03 | 0.12 | 0.03 | 0.03 | 0.11 | 0.03 | 0.03 | 0.13 |
| **Fixed Surface Models** | | | | | | | | | |
| C5ND | 0.85 | 0.91 | 4.45 | 0.91 | 0.91 | 4.68 | 0.9 | 0.96 | 4.74 |
| C6 | 0.06 | 0.06 | 0.30 | 0.06 | 0.06 | 0.31 | 0.06 | 0.06 | 0.32 |

### 2.5.3 Transition Probabilities

The probability of remaining at the surface as a C5ND for the "Low Food Surface" and "High Food Surface" models depends on the critical values of Phytoplankton Color Index, $C_l$ and $C_h$. In the "High Food Surface" model, PCI values are below the optimized values of $C_l$ and $C_h$ for all three cases. This means that, at any given time, the fraction of C4 that develop into C5ND is always $p = p_l = 0.1$ for both decades. Also, for the "All Differ" and "Fish Same" cases, the optimized values of these two parameters are almost equal implying almost an instantaneous shift between conditions.

For the "Low Food Transit" model, the critical PCI values which determine transition to C5ND are at the low range of PCI values in the 1980s and below the range of PCI values in the 1990s. The result is that, at least in the "All Differ" and "Fish Same" cases, C4s are more likely to develop into C5ND in the 1980s. In the 1990s only 10% transition into C5ND at any given time for the "All Differ" and "Food Same" cases. A small fraction remain at the surface as C5ND in the "Fish Same" case between days 150-170, but most transition from C4 to C5D. Figure 2.9 shows the comparison of food dependent transition for the "Low Food Surface" model for all three cases. For the "All Differ" case the optimized values for $C_l$ and $C_H$ are almost identical implying an almost instantaneous jump from one condition to the next as phytoplankton abundance increases.

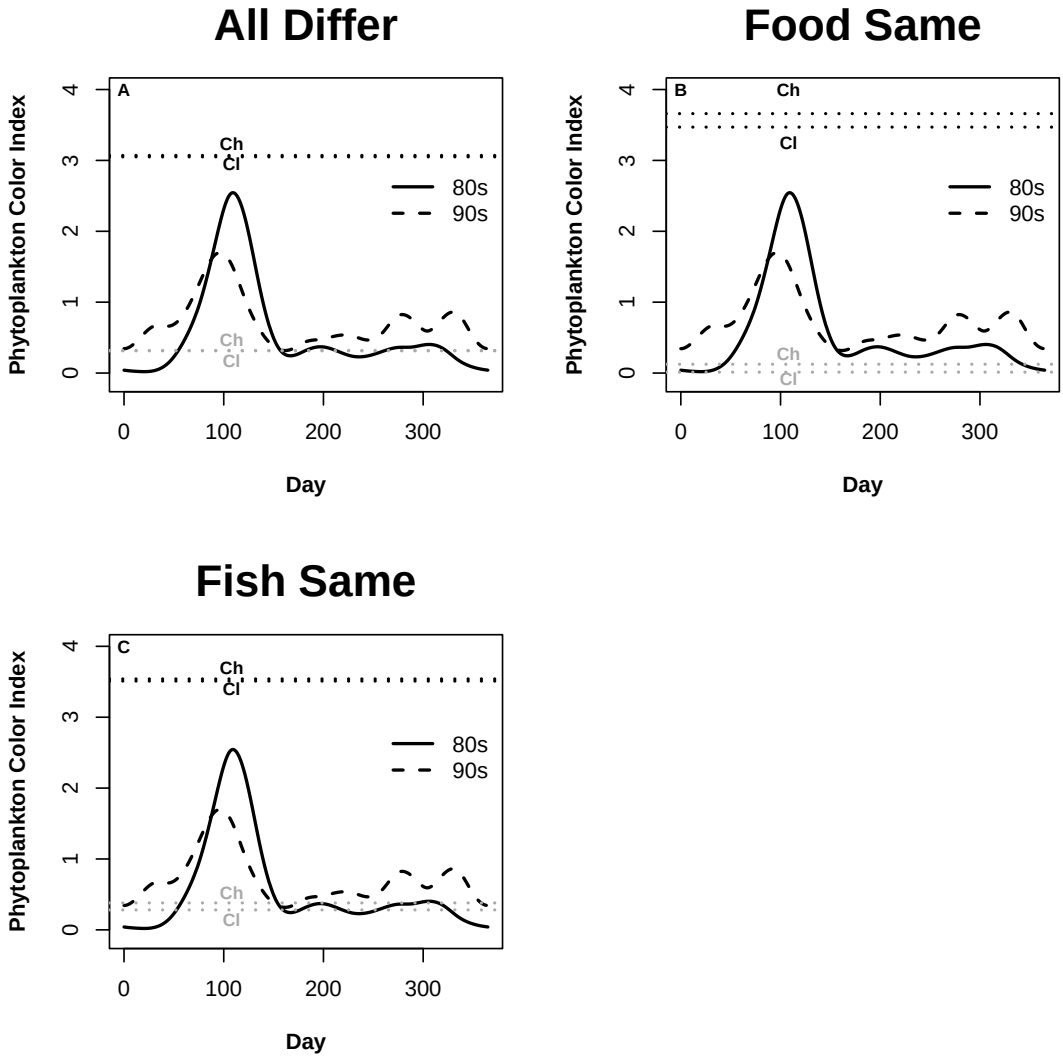


Figure 2.8: Each panel shows the optimized values of $C_l$ and $C_h$ for the "Low Food Surface" and "High Food Surface" models graphed against phytoplankton abundance (PCI). The average annual PCI is represented by a solid black line for the 1980s and a dashed black line for the 1990s. The optimized values are represented by gray dotted lines for the "Low Food Surface" model and black dotted lines for the "High Food Surface" model. Results are shown for the three cases: "Fish Differ" (**A**), "Food Same" (**B**) and "Fish Same" (**C**).
Specific values for $C_l$ and $C_h$ can be found in Table 2.4.

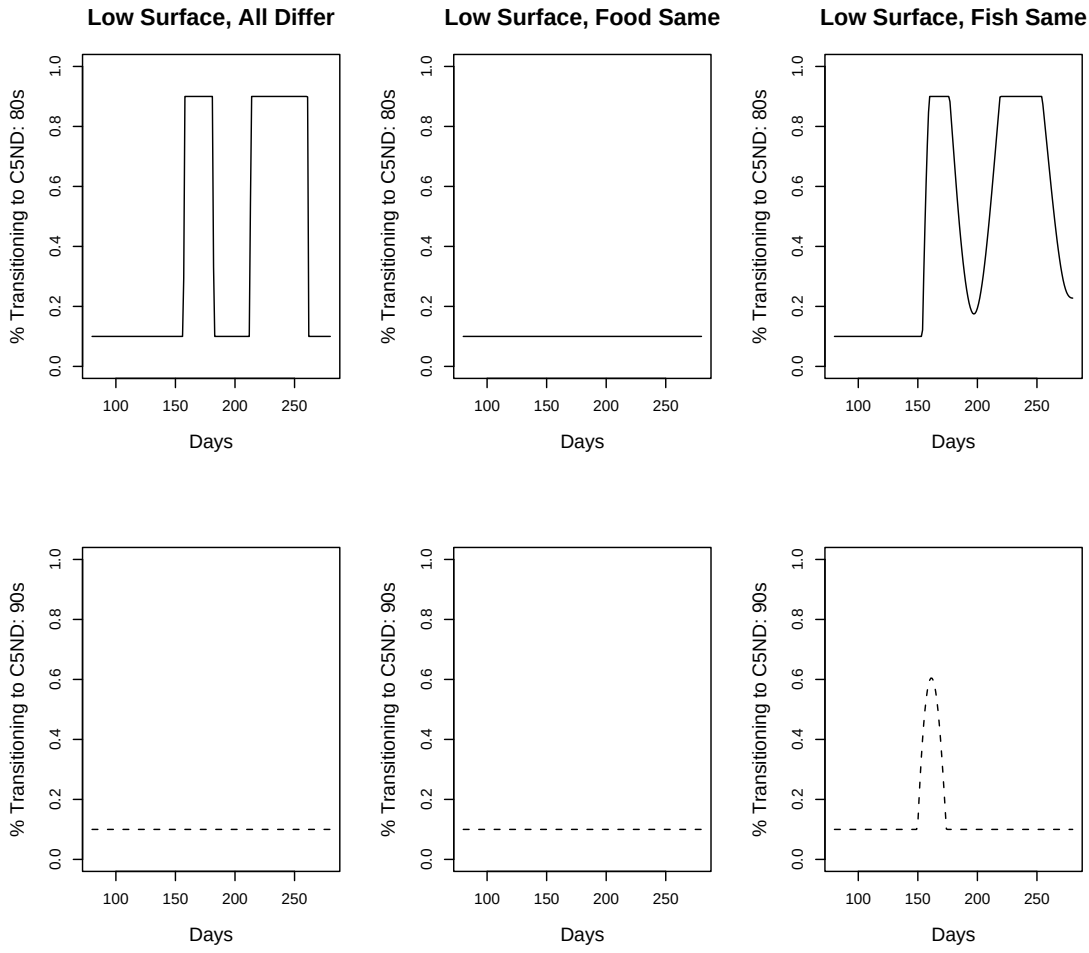


Figure 2.9: Transition Probability over time for the "Low Food Surface" model across all three cases ("All Differ", "Food Same", "Fish Same"). The top three panels from left to right give the transition probabilities in each case for the 80s. The bottom three panels give the transition probabilities for each case in the 90s.

## 2.6 Discussion

Both AIC and BIC analysis indicated that the "Low Food Surface, All Differ" scenario had the greatest ability to explain the decrease in late-stage *Calanus finmarchicus* in the 1990s. All other scenarios had a $\Delta$AIC $>$ 20 which suggests that they had little explanatory power in describing the data. Consequently, it is likely that both bottom-up and top-down controls were important in determining the shift in annual abundance patterns of *C. finmarchicus* in the 1990s. Furthermore, our results suggest that development from C4 to C5ND is best explained by insufficient lipid stores to make it into diapause (31).

It is not completely surprising that the "Low Food Surface, All Differ" model appears to be the best fit to the data overall; it is the only hypothesis of the three tested that would explain how an increase in food abundance could lead to a decrease in the surface populations of late-stage *Calanus*. During the 1990s, the spring phytoplankton bloom occurred earlier and lasted longer. More importantly, the fall bloom was significantly larger on average than in the previous decade. Under the definition for transition probability in the "Low Food Surface" model, this would lead to an increase in the fraction of C4 transitioning into diapause when food is more abundant. Although increased food abundance occurs both during the January-March as well as from July-December during the 1990s, C4s are most present between days 80-280 (see Figure 2.3). This implies that changes in phytoplankton abundance are more likely to affect transition into the later stages in the fall, according to the "Low Food Surface" model.

Data for the diapause class is not available from the CPR survey conducted by NMFS to determine how abundance for this class changed during the 1990s. The Gulf of Maine is not a closed ecosystem and changes in influx from adjacent waters

(e.g. Scotian Shelf) are a significant source of variation in *Calanus finmarchicus* abundance (39). Research by (21; 25) suggest that changes in water circulation patterns during the 1990s resulted in a decrease in *C. Finmarchicus* being advected off the Scotian Shelf. This might explain the decline in the late-stage *Calanus* population in January that initiate the first generation in the year. However, according to (15), the increase in *Calanus* spring reproduction during the 1990s compensated for the decrease in the resting population at the beginning of the year. This is reflected in the data by the fact that the 1980s and the 1990s abundances are essentially the same by day 100. Changes in advection might have resulted in decreases in late-stage *Calanus* in the beginning of the year in the 1990s; but it certainly does not explain why late-stage abundance dropped again during the late summer and early fall despite having recovered to the levels of the 1980s by late spring.

Given how the definition of food-dependent transition might affect the decrease in late-stage *Calanus* in the fall, it is clear how bottom-up processes might contribute to the annual abundance patterns of the 1990s. Yet, the scenario that included only changes in food ("Low Food Surface, Fish Same") was a much worse fit to the data than the scenario which assumed that changes in both herring and phytoplankton occurred during the 1990s. The AIC results suggest that the patterns observed in the data cannot be captured without the inclusion of increased herring abundance in the 1990s. From comparing the results in Figure 2.5, adding changes in herring abundance seems most important for capturing the decrease in fall *Calanus* abundance.

One thing to note is that including increased herring abundance in the 1990s potentially overestimates the decrease in *Calanus* abundance in the spring. Annual

abundance patterns for herring were estimated based on the ELMR database. For construction of the models, we made the simplifying assumption that the ELMR data was on a linear scale. Assuming linearity in this scale might have led to an over-estimate of abundance in the early part of the year from January-April. From December-March, herring abundance is given a score of 3 (Common) according the ELMR survey relative to their peak summer abundance of 5 (Highly Abundant). Allowing the ELMR scale to reflect linear changes in abundance, we assumed that the abundance in winter was approximately half the abundance at peak values in the summer. In reality, a log scale might be a better reflection of how monthly abundance patterns were determined in this data set. The non-linearity of this scale should be taken into account in future work on this system.

Another impact of bottom-up processes not addressed in our model is the role that changes in zooplankton abundance had on recruitment of herring into adulthood. The recovery of herring which resulted in such large adult classes during this period was, in part, a result of an increase in larval herring recruitment (53). This increased recruitment rate has been attributed to the abnormally high fall bloom throughout the decade which led to larger-than-normal populations of small zooplankton species such as *Oithona*, *Pseudocalanus*, and *Centropages typicus* which dominate the fall bloom (48). Adult herring spawn between July-November in the Gulf of Maine (51) and generally, after hatching, larvae are exposed to extremely low food conditions (20). The secondary bloom in autumn months which gave rise to increased abundances of smaller zooplankton most likely allowed larval herring to survive the winter at higher rates than in the previous decade. In other words, bottom-up processes, which aided the growth of small zooplankton and larval herring, could then lead to top-down control of the larger, *C. finmarchicus* due to increased presence of adult herring.

Much of the research that has been conducted up to this point to explain declines in late-stage *C. finmarchicus* has focused primarily on the role of physiological and bottom-up processes. There is a long-held belief that bottom-up process tend to drive open-ocean systems to a much larger extent than top-down processes (12). Although there are numerous examples of top-down control in freshwater systems and in the rocky intertidal (38; 47), there is less evidence in support of predatory control in open ocean ecosystems (50; 4). However, over the last decade, there has been mounting evidence for the importance of top-down control. In a recent study from the Barents Sea, for example, top-down control of zooplankton by pelagic fish was demonstrated (13). In another study by Maes et al. (2005), on the impact of juvenile herring and sprat on estuarine zooplankton, it was found that both fish exerted strong top-down control on the plankton populations (35). It has been hypothesized that the sensitivity of an ecosystem to top-down controls can depend quite heavily on the species diversity in a given region and that an ecosystem which is species-poor is much more likely to be mediated by top-down processes (18; 4).

Our results suggest that increased herring presence in the 1990s might have played an important role in the decline of late-stage *C. finmarchicus* during this period. It is interesting then to consider how increased herring presence in the Gulf of Maine might have affected other predators in the region. Humpback whales for example, which prey on herring, benefited by the shift in herring abundance. The North Atlantic right whale on the other hand, which also prey on *C. finmarchicus* saw a decrease in abundance throughout this decade. All of the known feeding grounds for the right whales are in the Gulf of Maine and adjacent Scotian Shelf and their primary food source is late-stage *C. finmarchicus* (22). The decline of late-stage *C. finmarchicus* in the 1990s is significant in terms of right whales because

the oil reserves found in the later stages of diapausing C4 and C5 *C. finmarchicus* are a critical nutritional source for the whales. During the 1980s the average length of time between new calves was 2-3 years, but this number increased to 4-6 years in the following decade, potentially as a result of malnutrition. According to (10), yearly population growth rate declined from 1.05 in 1980 to 0.98 in 1994. Several recent studies, have connected the variability in *C. finmarchicus* abundance to the declines in right whale reproduction (34; 24; 22). In support of this link, right whales showed a shift in feeding ground in the 1990s, most likely as a result of the decrease in late-stage *C. finmarchicus* in this region. Interestingly, data collected since 2002 on right whale fecundity has shown a slow recovery of reproductive rates back to levels found during the 1980s. Our results suggest that the increased presence of adult herring during the 1990s might explain, at least in part the food limitation experienced by right whales at that time.

The study presented in this paper is a simplification of a complicated system. We do not explicitly model changes in phytoplankton and herring abundance over time, nor do we include other small zooplankton species which are potentially important for herring recruitment. Clearly, there is room for further investigation on the relative importance of top-down versus bottom-up control on *C. finmarchicus* abundance. Yet, despite the simplicity of the models, the best-fit model accurately capture changes in seasonal patterns of abundance between the 1980s and the 1980s. Our results indicate that in order to fully understand the ecosystem observed in the 1990s, both bottom-up and top-down processes must be considered when exploring the variability of *C. finmarchicus* abundance.

# BIBLIOGRAPHY


[1] H. Akaike. A new look at the statistical model identification. *IEEE Transactions on Automatic Control*, 19:716–723, 1974.

[2] S. D. Batten, A. W. Walne, M. Edwards, and S. B. Groom. Phytoplankton biomass from continuous plankton recorder data: an assessment of the phytoplankton colour index. *Journal of Plankton Research*, 25:697–702, 2003.

[3] R. S. Batty, J. H. S. Blaxter, and D. A. Libby. Herring (*Clupea harengus*) filter-feeding in the dark. *Marine Biology*, 91:371–375, 1986.

[4] J. K. Baum and B. Worm. Cascading top-down effects of changing oceanic predator abundances. *Journal of Animal Ecology*, 78:699–714, 2009.

[5] M. F. Baumgartner, T. V. N. Cole, R. G. Campbell, G. J. Teegarden, and E. G. Durbin. Associations between North Atlantic right whales and their prey, *Calanus finmarchicus*, over diel and tidal time scales. *Marine Ecology Progress Series*, 264:155–166, 2003.

[6] B. M. Bolker. *Ecological Models and Data in R.* Princeton University Press, 2008.

[7] M. W. Brown and S. D. Kraus. COSEWIC assessment and update status report on the North Atlantic right whale *Eubalaena glacialis* in Canada. Committee on the Status of Endangered Wildlife in Canada. Status report, NOAA fisheries/Fisheries and Oceans Canada, 2003.

[8] K. P. Burnham and D. R. Anderson. *Model Selection and Multimodel Inference: A Practical Information-Theoretic Approach.* Springer-Verlag, 2002.

[9] R. G. Campbell, M. M. Wagner, G. J. Teegarden, C. A. Boudreau, and E. G. Durbin. Growth and development of *Calanus finmarchicus* in the laboratory. *Marine Ecology Progress Series*, 221:161–183, 2001.

[10] H. Caswell, M. Fujiwara, and S. Brault. Declining survival probability threatens the North Atlantic right whale. *Proceedings of the National Academy of Sciences*, 96:3308–3313, 1999.

[11] R. E. Cohen and R. G. Lough. Prey field of larval herring *Clupea harengus* on a continental shelf spawning area. *Marine Ecology Progress Series*, 10:211–222, 1983.

[12] D. H. Cushing. *Marine Ecology and Fisheries*. Cambridge University Press, 1975.

[13] P. Dalpadado and H. R. Skoldal. Abundance, maturity and growth of the krill species *Thysanoessa inermis* and *T. longicaudata* in the Barent Sea. *Marine Ecology Progress Series*, 144:175–183, 1996.

[14] E. Darbyson, D. P. Swain, D. Chabot, and M. Castonguay. Diel variation in feeding rate and prey composition of herring and mackerel in the southern Gulf of St Lawrence. *Journal of Fish Biology*, 63:1235–1257, 2003.

[15] E. G. Durbin, R. G. Campbell, M. C. Casas, M. D. Ohman, B. Niehoff, J. Runge, and M. Wagner. Interannual variation in phytoplankton blooms and zooplankton productivity and abundance in the Gulf of Maine during winter. *Marine Ecology Progress Series*, 254:81–100, 2003.

[16] K. Eiane, D. L. Aksnes, M. D. Ohman, S. Wood, and M. B. Martinussen. Stage-specific mortality of it Calanus spp. under different predation regimes. *Limnology and Oceanography*, 47:636–645, 2002.

[17] K. T. Frank, B. Petrie abd J. S. Choi, and W. C. Leggett. Trophic cascades in a formerly cod-dominated ecosystem. *Science*, 308:1621–1623, 2005.

[18] K. T. Frank, B. Petrie, and N. L. Shackell. The ups and downs of trophic control in continental shelf ecosystems. *Trends in Ecology and Evolution*, 22:636–645, 2007.

[19] R. N. Gibson and I. A. Ezzi. Effect of particle concentration on filter- and particulate-feeding in the herring *Clupea harengus*. *Marine Biology*, 88:109–116, 1985.

[20] J. J. Graham, D. K. Stevenson, and K. M. Sherman. Relation between winter temperature and survival of larval Atlantic herring along the Maine coast. *Transactions of the American Fisheries Society*, 119:730–740, 1990.

[21] C. H. Greene and A. J. Pershing. The response of *Calanus finmarchicus* populations to climate variability in the Northwest Atlantic: Basin-scale forcing associated with the North Atlantic Oscillation (NAO). *ICES Journal of Marine Science*, 57:15361544, 2001.

[22] C. H. Greene and A. J. Pershing. Climate and the conservation biology of North Atlantic right whales: The right whale at the wrong time? *Frontiers in Ecology and the Environment*, 2:29–34, 2004.

[23] C. H. Greene and A. J. Pershing. Climate drives sea change. *Science*, 315:1084–1085, 2007.

[24] C. H. Greene, A. J. Pershing, R. D. Kenney, and J. W. Jossi. Impact of climate variability on the recovery of endangered North Atlantic right whales. *Oceanography*, 16:98–103, 2003.

[25] C.H. Greene, A.J. Pershing, A. Conversi, B. Planque, C. Hannah, D. Sameoto, E. Head, P.C. Smith, P.C. Reid, J. Jossi, D. Mountain, M.C. Benfield, P.H. Wiebe, and E. Durbin. Trans-Atlantic responses of *Calanus finmarchicus* populations to basin-scale forcing associated with the North Atlantic Oscillation. *Progress in Oceanography*, 58:301–312, 2003.

[26] D. N. Gregory. Climate: A database of temperature and salinity observations for the Northwest Atlantic. Canadian Science Advisory Secritariat Research Document 2004/075, Department of Fisheries and Oceans, 2004.

[27] G.D. Grossman, R. E. Ratajczak, J. T. Petty, M. D. Hunter, J. T. Peterson, and G. Grenouillet. Population dynamics of mottled sculpin (pisces: Cottidae) in a variable environment: information theoretic approaches. *Ecological Monographs*, 76:217–234, 2006.

[28] A. Hind, W. S. C. Gurney, M. Heath, and A. D. Bryant. Overwintering strategies in *Calanus finmarchicus*. *Marine Ecology Progress Series*, 193:95–107, 2000.

[29] H. J. Hirche. The reproductive biology of the marine copepod, *Calanus finmarchicus* a review. *Ophelia*, 44:111–128, 1996.

[30] A. G. Hirst and T. Kirboe. Mortality of marine planktonic copepods: global rates and patterns. *Marine Ecology Progress Series*, 230:195–209, 2002.

[31] C. L. Johnson, A. W. Leising, J. A. Runge, E. J. H. Head, P. Pepin, S. Plourde, and E. G. Durbin. Characteristics of *Calanus finmarchicus* dormancy patterns in the Northwest Atlantic. *ICES Journal of Marine Sciences*, 65:339–350, 2007.

[32] J. W. Jossi and J. R. Goulet. Zooplankton trends: US northeast shelf ecosystem and adjacent regions differ from northeast Atlantic and North sea. *ICES Journal of Marine Science*, 50:303–313, 1993.

[33] J. Kane. The feeding habits of co-occuring cod and haddock larvae from Georges Bank. *Marine Ecology Progress Series*, 16:9–20, 1984.

[34] R. D. Kenney, C. A. Mayo, and H. E. Winn. Migration and foraging strategies at varying spatial scales in western North Atlantic right whales: a review of hypotheses. *Journal of Cetacean Research Management*, 2S:251–260, 2001.

[35] J. Maes, M. Tackx, and K. Soetaert. The predation impact of juvenile herring *Clupea harengus* and sprat *Sprattus sprattus* on estuarine zooplankton. *Hydrobiologia*, 540:225–235, 2005.

[36] K. McCann. Density-dependent coexistence in fish communities. *Ecology*, 79:2957–2967, 1998.

[37] C. J. Meise and J. E. OReilly. Spatial and seasonal patterns in abundance and age-composition of *Calanus finmarchicus* in the Gulf of Maine and on Georges Bank: 1977-1987. *Deep-Sea Research II*, 43:1473–1501, 1996.

[38] B.A. Menge. Top-down and bottum-up community regulation in marine rocky intertidal habitats. *Journal of Experimental Marine Biology and Ecology*, 250:257–289, 2000.

[39] MERCINA. Gulf of Maine/Western Scotian Shelf ecosystems respond to changes in ocean circulation associated with the North Atlantic Oscillation. *Oceanography*, 14:76–82, 2001.

[40] C. B. Miller, D. R. Lynch, F. Carlotti, W. Gentleman, and C. V. W. Lewis. Coupling of an individual-based population dynamic model of *Calanus fin-*

*marchicus* to a circulation model for the Georges Bank region. *Fisheries Oceanography*, 7:219–234, 1998.

[41] D. B. Mountain. Variability of the water properties in NAFO subareas 5 and 6 during the 1990s. *Journal of Northwest Atlantic Fisheries Science*, 34:103–112, 2004.

[42] R. A. Myers and J. A. Runge. Predictions of seasonal natural mortality rates in a copepod population using life-history theory. *Marine Ecology Progress Series*, 11:189–194, 1983.

[43] D. M. Nelson and M. E. Monaco. National overview and evolution of NOAA's Estuarine Living Marine Resources (ELMR) program. Noaa technical memorandum nos nccos ccma, 144, US Deptartment of Commerce, National Oceanic and Atmospheric Administration, National Ocean Service, National Centers for Coastal Ocean Science, Center for Coastal Monitoring and Assessment, 2000.

[44] M. D. Ohman, K. Eiane, E. G. Durbin, J. A. Runge, and H.-J. Hirche. A comparative study of *Calanus finmarchicus* mortality patterns at five localities in the North Atlantic. *ICES Journal of Marine Science*, 61:687–697, 2004.

[45] W. J. Overholtz. The Gulf of Maine - Georges Bank Atlantic herring *Clupea harengus*: Spatial pattern analysis of the collapse and recovery of a large marine fish complex. *Fisheries Research*, 57:237–254, 2002.

[46] W. J. Overholtz, L. D. Jacobson, G. D. Melvin, M. Cieri, M. Power, D. Libby, and K. Clark. Stock assessment of the Gulf of Maine - Georges Bank Atlantic herring complex, 2003. Northeast fisheries science center reference document 04-06, Northeast Fisheries Science Center, 2003.

[47] R. T. Paine. A note on trophic complexity and community stability. *American Naturalist*, 103:91–93, 1969.

[48] A. J. Pershing, C. H. Greene, J. W. Jossi, L. OBrien, J. K. T. Brodziak, and B. A. Bailey. Interdecadal variability in the Gulf of Maine zooplankton community, with potential impacts on fish recruitment. *ICES Journal of Marine Science*, 62:1511–1523, 2005.

[49] B. Planque and S. D. Batten. *Calanus finmarchicus* in the North Atlantic: the year of it Calanus in the context of interdecadal change. *ICES Journal of Marine Science,*, 57:1528–1535, 2000.

[50] P. C. Reid, E. J. V. Battle, S. D. Batten, and K. M. Brander. Impacts of fisheries on plankton community structure. *ICES Journal of Marine Science,*, 57:495–502, 2000.

[51] M. Sinclair and M. J. Tremblay. Timing of spawning of Atlantic herring (*Clupea harengus harengus*) populations and the match-mismatch theory. *Canadian Journal of Fisheries and Aquatic Sciences*, 41:1055–1065, 1984.

[52] D. C. Speirs, W. C. Gurney, M. R. Heath, W. Horbelt, S. N. Wood, and B. A. de Cuevas. Ocean-scale modelling of the distribution, abundance, and seasonal dynamics of the copepod *Calanus finmarchicus*. *Marine Ecology Progress Series*, 313:173–192, 2006.

[53] Transboundary Resource Assessment Committee. Gulf of Maine-Georges Bank herring stock complex. Trac status report 2006/01, NOAA fisheries/Fisheries and Oceans Canada, 2006.

[54] K. F. Wishner, J. R. Schoenherr, R. Beardsley, and C. S. Chen. Abundance, distribution and population structure of the copepod *Calanus finmarchicus*

in a springtime right whale feeding area in the southwestern Gulf of Maine. *Continental Shelf Research*, 15:475–507, 1995.